Competition between Steric and Electronic Control of Structure in $Ru(CO)_2L_2L'$ Complexes

Masamichi Ogasawara,*,† Feliu Maseras,‡ Nuria Gallego-Planas,‡ Kazumori Kawamura,†,§ Kazuhiko Ito,†,§ Koichiro Toyota,†,§ William E. Streib,† Sanshiro Komiya,†,∥ Odile Eisenstein,‡ and Kenneth G. Caulton†,⊥

Department of Chemistry and Molecular Structure Center, Indiana University, Bloomington, Indiana 47405-4001, and LSDSMS (UMR 5636), Case Courier 14, Bâtiment 15, Université de Montpellier 2, 34095 Montpellier Cedex 5, France

Received February 3, 1997[⊗]

Magnesium reduction of $RuCl_2(CO)_2L_2$ in the presence of equimolar L in THF gives $Ru(CO)_2L_3$ (L = PPh_3 (**1**), $PMePh_2$ (**2**), PEt_3 (**3**), P^iPr_2Me (**4**)). The corresponding reduction of $RuCl_2(CO)_2(PEt_3)_2$ in the presence of equimolar L′ (L′ = P(2-furyl)$_3$ (**5**) or $AsPh_3$ (**6**)) gives $Ru(CO)_2(PEt_3)_2L'$ but gives a mixture of $Ru(CO)_2(PEt_3)_{3-n}L_n$ (n = 0−3) species when L′ = PPh_3. Comparisons show that **3** or **5** reacts slowly with L″ = $(H)_2$, CO, or PhC≡CPh to form $Ru(CO)_2L''(PEt_3)_2$ and free PEt_3 or P(2-furyl)$_3$ but *rapidly* with **4** or **6** to give the analogous products. The reaction of PhC≡CPh with $Ru(CO)_2(PEt_3)_2L'$ is faster for L′ = PEt_3 than for P(2-furyl)$_3$. All of these reactions are proposed to take place by preliminary ligand loss of L′, this being slower for **3** and **5** than for **1**, **4**, and **6**. Reaction of O_2 with complexes containing the readily dissociated L′ species gives simply $Ru(\eta^2\text{-}O_2)(CO)_2L_2$, but for $Ru(CO)_2(PEt_3)_3$, this is accompanied by an apparent bimolecular electron transfer involving the intact complex to give $Ru(CO)(CO_3)(PEt_3)_3$. X-ray structure determinations of $Ru(CO)_2(PEt_3)_3$ (bis equatorial CO in trigonal bipyramid (TBP)), $Ru(CO)_2(P^iPr_2Me)_3$ (two isomers: bis axial CO in TBP and also square pyramidal), and $Ru(\eta^2\text{-}PhCCPh)(CO)_2(PEt_3)_2$ (*cis* carbonyls and *trans* phosphines) are reported. It is shown that all of the $Ru(CO)_2L_3$ species exist in solution as two isomers in rapid equilibrium. *Ab initio* MP2 calculations on the unhindered $Ru(CO)_2(PH_3)_3$ model shows a preference for a trigonal bipyramidal structure with only a weak preference for CO to be at the equatorial site. It is shown that this pattern cannot be generalized to all π-acid ligands since ethylene is calculated to have a strong preference for an equatorial site in a TBP. Integrated quantum chemical and molecular mechanics calculations on $Ru(CO)_2(PEt_3)_3$ and $Ru(CO)_2(P^iPr_2Me)_3$ give structures in excellent agreement with the X-ray results and confirm that the geometry and relative energetic preference for the observed structural isomers is strongly influenced, or even dominated by, the steric effect of the phosphine ligands.

Introduction

Many $Ru(CO)_5$ derivatives of the type $Ru(CO)_4L$ and $Ru(CO)_3L_2$ have been reported, and they comprise the core of zero-valent ruthenium chemistry, together with clusters derived from $Ru_3(CO)_{12}$.[1] In the 1970s, Roper and co-workers reported the synthesis of $Ru(CO)_2(PPh_3)_3$ by a multistep route (eq 1).[2] The most valuable feature of this complex is its unusual willingness to react by loss of one PPh_3 ligand to make a range of $Ru(CO)_2(PPh_3)_2L_n$ complexes containing unusual ligands L (L = CF_2,[3] S_2,[4] etc.). Roper suggested that this

$$\begin{aligned}
&RuHCl(CO)(PPh_3)_3 + AgClO_4 + 2MeCN \rightarrow \\
&\quad [RuH(CO)(MeCN)_2(PPh_3)_2]ClO_4 + AgCl + PPh_3 \\
&[RuH(CO)(MeCN)_2(PPh_3)_2]ClO_4 + CO \rightarrow \\
&\quad ([RuH(CO)_2(MeCN)(PPh_3)_2]ClO_4) \\
&\quad\quad \downarrow + PPh_3 \\
&\quad\quad [RuH(CO)_2(PPh_3)_3]ClO_4 \\
&[RuH(CO)_2(PPh_3)_3]ClO_4 + {}^t\!BuOK \rightarrow \\
&\quad Ru(CO)_2(PPh_3)_3 + KClO_4 + {}^t\!BuOH \quad (1)
\end{aligned}$$

phosphine dissociation presumably occurred because three bulky PPh_3 ligands in one molecule are sterically unfavorable. The implication was that this molecule reacts by a dissociative mechanism, in spite of the rarity (and thus presumed high energy) of isolable 16-electron Ru(0) compounds. We reported recently the reduction of *cis*,*cis*,*trans*-$RuCl_2(CO)_2(P^tBu_2Me)_2$ with Mg in THF to give unsaturated $Ru(CO)_2(P^tBu_2Me)_2$.[5] This molecule may be a model of the probable "high-energy intermedi-

† Indiana University.
‡ Université de Montpellier.
§ Temporary visiting researchers at Indiana University (1995) on leave from the Department of Chemistry, Hiroshima University, Japan.
∥ On sabbatical leave from the Department of Applied Chemistry, Tokyo University of Agriculture and Technology, Japan.
⊥ E-mail: caulton@indiana.edu; eisenst@lsd.univ-montp2.fr.
⊗ Abstract published in *Advance ACS Abstracts,* April 1, 1997.

(1) Bennett, M. A.; Bruce, M. I.; Matheson, T. W. *Comprehensive Organometallic Chemistry*; Pergamon Press: New York, 1982; Vol. 4, p 691.
(2) Cavit, B. E.; Grundy, K. R.; Roper, W. R. *J. Chem. Soc., Chem. Commun.* **1972**, 60.
(3) Clark, G. R.; Hoskins, S. V.; Jones, T. C.; Roper, W. R. *J. Chem. Soc., Chem. Commun.* **1983**, 719.
(4) Clark, G. R.; Russell, D. R.; Roper, W. R.; Walker, A. *J. Organomet. Chem.* **1977**, *136*, C1.

S0276-7333(97)00077-0 CCC: $14.00

ate" from Roper's complex. However, $Ru(CO)_2(P^tBu_2Me)_2$ shows unusual stability (i.e., persistence).[5,6] The complex $Ru(CO)_2(P^tBu_2Me)_2$ also represents the only X-ray structurally characterized d^8 four-coordinate complex whose structure is *not* planar. *Ab initio* calculations clarified that the bent OC−Ru−CO unit in the complex is stabilizing the molecule and that its structure is not due to the bulkiness of the P^tBu_2Me ligands because calculations on the model compound $Ru(CO)_2(PH_3)_2$ reproduced quantitatively the experimental angles at the metal. Successful isolation of $Ru(CO)_2(P^tBu_2Me)_2$ as a persistent complex suggests the possibility that dissociation of a phosphine ligand L from $Ru(CO)_2L_3$, generating $Ru(CO)_2L_2$, is *not* so thermodynamically unfavorable, even though the phosphine ligands L are not sterically demanding.

In spite of its attractive reactivity, $Ru(CO)_2(PPh_3)_3$ remains as the only example of an isolated $Ru(CO)_2L_3$ derivative.[7] Presumably, some of the original reaction steps are not applicable to other analogous complexes with different phosphines due to its complicated synthetic route. In this paper, we describe a very convenient new synthesis of Roper's complex $Ru(CO)_2(PPh_3)_3$, which has also enabled us to produce a range of $Ru(CO)_2L_2L'$ species involving mixed phosphine[8] and phosphine/arsine complexes ($L \neq L'$) with a range of steric and electronic properties. This achievement also gives us an opportunity to clarify the prediction of accessible $Ru(CO)_2L_2$ species mentioned above. Furthermore, in the course of the investigation, we found an interesting relationship between the structures of the complexes and the steric properties of the phosphines. We report here on our observations. Part of this work has been reported in a preliminary communication.[9]

Experimental Section

General. All manipulations were carried out using standard Schlenk and glovebox techniques under prepurified argon. Benzene, heptane, pentane, THF, and toluene were dried over sodium benzophenone ketyl, distilled, and stored in gastight solvent bulbs. Methanol and 2-methoxyethanol were degassed under vacuum and used without further purification. Benzene-d_6 and toluene-d_8 were dried over sodium metal and vacuum-distilled prior to use. Phosphines (PEt_3, $PMePh_2$, and PPh_3), triphenylarsine, and 1,2-dibromoethane were purchased from Aldrich Chemical Co. and used without purification. P^iPr_2Me was synthesized from P^iPr_2Cl (Aldrich) and MeLi, distilled, and stored under argon. Tris(2-furyl)phosphine was a generous gift from Professor Masahiko Saburi of Saitama Institute of Technology, Japan. Diphenylacetylene was purchased from Aldrich Chemical Co. and used after purifying by sublimation under reduced pressure. Gaseous reagents (H_2, O_2, and CO) were purchased from Air Products and used as received. Ruthenium trichloride hydrate was a generous loan from Johnson Matthey and used as received. $RuCl_2(CO)_2(PEt_3)_2$,[10] $RuCl_2(CO)_2(PMePh_2)_2$,[11] and $RuCl_2(CO)_2(PPh_3)_2$[12] were synthesized as reported. ^1H (300 MHz) NMR spectra were recorded on a Varian XL300 spectrometer. ^{31}P NMR spectra were obtained on a Nicolet NT-360 spectrometer at 146 MHz or on a Varian XL300 spectrometer at 122 MHz. ^1H NMR chemical shifts are reported in ppm downfield of tetramethylsilane, using residual solvent resonances as internal standards. ^{31}P NMR chemical shifts are relative to an external standard, 85% H_3PO_4. Infrared spectra were recorded on a Nicolet 510P FT-IR spectrometer. Elemental analyses were performed on a Perkin-Elmer 2400 CHNS/O Elemental Analyzer at the Chemistry Department, Indiana University.

***cis,cis,trans*-$RuCl_2(CO)_2(P^iPr_2Me)_2$.** Carbon monoxide was passed through a solution of ruthenium trichloride hydrate (1.50 g, 6.5 mmol) in 2-methoxyethanol (35 mL) at 130 °C until the solution color changed to pale yellow. After a small amount of insoluble material was filtered away, P^iPr_2Me (1.85 g, 14 mmol) was added and the solution was refluxed for 10 min. The solution was concentrated to *ca.* 8 mL under reduced pressure and cooled to −20 °C, yielding two crops of white crystals; yield 2.59 g (5.3 mmol, 81%). ^1H NMR (C_6D_6, 23 °C): δ 0.92 (dvt, $J_{HP} = J_{HH} = 7.2$ Hz, 12H, PCCH_3), 1.20 (dvt, $J_{HP} = J_{HH} = 7.2$ Hz, 12H, PCCH_3), 1.47 (vt, $J_{HP} = 3.9$ Hz, 6H, PCH_3), 2.19 (m, 4H, PCHMe$_2$). $^{31}P\{^1H\}$ NMR (C_6D_6, 23 °C): δ 28.7 (s). IR (C_6D_6): ν_{CO} 2033, 1966 cm^{-1}. Anal. Calcd for $RuC_{16}H_{34}Cl_2O_2P_2$: C, 39.03; H, 6.96. Found: C, 39.26; H, 7.07.

Activation of Magnesium Turnings. The typical procedure to generate the activated magnesium turnings is followed. Magnesium turnings (25 mg, 1.03 mmol) and THF (1 mL) were placed in a Schlenk flask, and 1,2-dibromoethane (20 μL, 0.23 mmol) was added via syringe. The mixture was gently stirred until the evolution of ethylene ceased, to give the activated magnesium (0.80 mmol). This magnesium was used immediately in another reaction without further treatment.

$Ru(CO)_2(PPh_3)_3$ (1). Magnesium turnings (55 mg, 2.27 mmol) were activated with 1,2-dibromoethane (41 μL, 0.47 mmol) in THF (1.5 mL) in a Schlenk flask. To the flask, a mixture of *cis,cis,trans*-$RuCl_2(CO)_2(PPh_3)_2$ (1.36 g, 1.80 mmol) and triphenylphosphine (0.49 g, 1.87 mmol) in THF (40 mL) was added by means of cannula transfer. The mixture was stirred at 60 °C, until all of the magnesium was consumed (*ca.* 10 h). During this period, the color of the solution changed from colorless to pale yellow. The volatiles were removed, and the pale yellow residue was extracted with benzene (40 mL × 4). After the insoluble material was filtered away, the solution was concentrated to *ca.* 20 mL. Addition of methanol (*ca.* 100 mL) to this solution gave the yellow-orange precipitate. Washing with MeOH and pentane gave the title compound in pure form; yield 1.55 g (1.62 mmol, 92%). All of the spectroscopic data are consistent with those reported previously.[2,13]

$Ru(CO)_2(PMePh_2)_3$ (2). A mixture of *cis,cis,trans*-$RuCl_2(CO)_2(PMePh_2)_2$ (300 mg, 0.48 mmol) and $PMePh_2$ (105 mg, 0.52 mmol) in THF (10 mL) was added to a THF suspension of activated magnesium (12 mg, 0.49 mmol) by means of cannula transfer. The mixture was stirred for 12 h at room temperature. During this period, the color of the solution changed from colorless to pale yellow. The volatiles were removed, and the yellow residue was extracted with hot heptane (15 mL × 4). The hot filtrate was cooled to room temperature to give two crops of yellow microcrystals; yield 299 mg (0.40 mmol, 83%). ^1H NMR (C_6D_6, 23 °C): δ 1.68 (m, 9H, PCH_3), 6.98 (m, 18H, *o*- and *p*-H), 7.53 (m, 12H, *m*-H). $^{31}P\{^1H\}$ NMR (C_6D_6, 23 °C): δ 28.3 (s). IR (C_6D_6): ν_{CO} 1896,

(5) Ogasawara, M.; Macgregor, S. A.; Streib, W. E.; Folting, K.; Eisenstein, O.; Caulton, K. G. *J. Am. Chem. Soc.* **1995**, *117*, 8869.
(6) Ogasawara, M.; Macgregor, S. A.; Streib, W. E.; Folting, K.; Eisenstein, O.; Caulton, K. G. *J. Am. Chem. Soc.* **1996**, *118*, 10189.
(7) There are very few reports of other $Ru(CO)_2(phosphine)_3$ complexes with some special phosphines. With tridentate chelate phosphines, see: (a) Siegl, W. O.; Lapporte, S. J.; Collman, J. P. *Inorg. Chem.* **1973**, *12*, 674. (b) Letts, J. B.; Mazanec, T. J.; Meek, D. W. *Organometallics* **1983**, *2*, 695. With PF_3, see: (c) Udovich, C. A.; Clark, R. J. *J. Organomet. Chem.* **1976**, *36*, 355.
(8) Two $Ru(CO)_2L_2L'$ complexes are reported as the ligand exchange products from $Ru(CO)_2(PPh_3)_3$, see: Bohle, D. S.; Roper, W. R. *Organometallics* **1986**, *5*, 1607.
(9) Ogasawara, M.; Maseras, F.; Gallego-Planas, N.; Streib, W. E.; Eisenstein, O.; Caulton, K. G. *Inorg. Chem.* **1996**, *35*, 7468.
(10) Lupin, M. S.; Shaw, B. L. *J. Chem. Soc. A* **1968**, 741.
(11) Gill, D. G.; Mann, B. E.; Shaw, B. L. *J. Chem. Soc., Dalton Trans.* **1973**, 311.
(12) Stephenson, T. A.; Wilkinson, G. *J. Inorg. Nucl. Chem.* **1966**, *28*, 945.
(13) Gaffney, T. R.; Ibers, J. A. *Inorg. Chem.* **1982**, *21*, 2851.

1844 cm^{-1}. Anal. Calcd for $RuC_{41}H_{39}O_2P_3$: C, 64.99; H, 5.19. Found: C, 64.86; H, 5.17.

Ru(CO)$_2$(PEt$_3$)$_3$ (3). A colorless solution of *cis*,*cis*,*trans*-$RuCl_2(CO)_2(PEt_3)_2$ (650 mg, 1.40 mmol) and PEt_3 (176 mg, 1.49 mmol) in THF (15 mL) was added to a THF suspension of activated magnesium (36 mg, 1.50 mmol) obtained as described above. The mixture continued to stir for 12 h at room temperature to give a yellow solution. The solvent was evaporated to dryness under reduced pressure. The residue was extracted with pentane (7 mL × 3), concentrated to *ca*. 3 mL, and cooled to −40 °C, yielding two crops of yellow crystals of the title compound (665 mg, 93%). ^{1}H NMR (C_6D_6, 23 °C): δ 1.06 (m, 27H, PCCH_3), 1.55 (m, 18H, PCH_2Me). ^{31}P{^{1}H} NMR (C_6D_6, 23 °C): δ 31.2 (s). IR (C_6D_6): ν_{CO} 1883, 1827 cm^{-1}. Anal. Calcd for $RuC_{20}H_{45}O_2P_3$: C, 46.96; H, 8.87. Found: C, 46.78; H, 8.60.

Ru(CO)$_2$(P^{i}Pr$_2$Me)$_3$ (4). A THF (15 mL) solution of *cis*,*cis*,*trans*-$RuCl_2(CO)_2(P^iPr_2Me)_2$ (800 mg, 1.62 mmol) and P^iPr_2Me (225 mg, 1.70 mmol) was added to a THF suspension of activated magnesium (44 mg, 1.80 mmol) in a Schlenk flask. The mixture was stirred for 12 h at room temperature. During this period, the color of the solution changed from colorless to light orange. The volatiles were removed, and the orange residue was extracted with pentane (5 mL × 3). The pentane solution was concentrated to *ca*. 2 mL and cooled to −40 °C, yielding orange crystals; yield 752 mg (1.36 mmol, 84%). ^{1}H NMR (C_6D_6, 20 °C): δ 1.09 (m, 18H, PCCH_3), 1.16 (m, 18H, PCCH_3), 1.22 (m, 9H, PCH_3), 1.89 (m, J_{HP} = 3.2 Hz, 6H, PC*H*Me$_2$). ^{31}P{^{1}H} NMR (C_6D_6, 20 °C): δ 40.0 (s). IR (Nujol): ν_{CO} 1865 cm^{-1}. Anal. Calcd for $RuC_{23}H_{51}O_2P_3$: C, 49.90; H, 9.28. Found: C, 49.68; H, 8.95.

Ru(CO)$_2$(PEt$_3$)$_2$[P(2-furyl)$_3$] (5). A THF (15 mL) solution of *cis*,*cis*,*trans*-$RuCl_2(CO)_2(PEt_3)_2$ (501 mg, 1.08 mmol) and tris-(2-furyl)phosphine (254 mg, 1.09 mmol) was added to a THF suspension of activated magnesium (27 mg, 1.11 mmol). The mixture was stirred for 12 h at room temperature to give a yellow solution with a small amount of Mg remaining. The solvent was removed under reduced pressure. The resulting solid was extracted with pentane (10 mL × 3), and the pentane extract was concentrated to *ca*. 5 mL. Cooling to −40 °C yielded yellow crystals; yield 560 mg (0.90 mmol, 83%). ^{1}H NMR (C_6D_6, 23 °C): δ 1.08 (m, 18H, PCCH_3), 1.52 (m, 12H, PCH_2Me), 6.08 (m, 3H, 5-furyl), 6.78 (m, 3H, 4-furyl), 7.19 (m, 3H, 3-furyl). ^{31}P{^{1}H} NMR (C_6D_6, 23 °C): δ −15.5 (t, J_{PP} = 24 Hz, 1P, P(2-furyl)$_3$), 35.6 (d, J_{PP} = 24 Hz, 2P, PEt_3). IR (C_6D_6): ν_{CO} 1900, 1844 cm^{-1}. Anal. Calcd for $RuC_{26}H_{39}O_5P_3$: C, 49.92; H, 6.28. Found: C, 49.84; H, 6.15.

Ru(CO)$_2$(PEt$_3$)$_2$(AsPh$_3$) (6). A THF (15 mL) solution of *cis*,*cis*,*trans*-$RuCl_2(CO)_2(PEt_3)_2$ (500 mg, 1.08 mmol) and triphenylarsine (340 mg, 1.11 mmol) was added to a THF suspension of activated magnesium (28 mg, 1.16 mmol). The mixture was stirred for 24 h at room temperature to give a dark brown solution with a small amount of Mg remaining. The solvent was removed under reduced pressure. The resulting solid was extracted with pentane (10 mL × 3), and the pentane extract was concentrated to *ca*. 3 mL. Cooling to −40 °C yielded tan colored crystals; yield 513 mg (0.73 mmol, 68%). ^{1}H NMR (C_6D_6, 20 °C): δ 0.97 (tvt, J_{PH} = J_{HH} = 7.5 Hz, 18H, PCCH_3), 1.32 (tvt, J_{HH} = 7.5 Hz, J_{PH} = 3.0 Hz, 12H, PCH_2Me), 7.03−7.09 (m, 9H, Ph), 7.82 (m, 6H, Ph). ^{31}P{^{1}H} NMR (C_6D_6, 20 °C): δ 33.8 (s). IR (C_6D_6): ν_{CO} 1889, 1833 cm^{-1}. Anal. Calcd for $RuC_{32}H_{45}AsO_2P_2$: C, 54.94; H, 6.48. Found: C, 55.00; H, 6.24.

Magnesium Reduction of RuCl$_2$(CO)$_2$(PEt$_3$)$_2$ with PPh$_3$. *cis*,*cis*,*trans*-$RuCl_2(CO)_2(PEt_3)_2$ (303 mg, 0.65 mmol) was reduced with activated magnesium (16 mg, 0.66 mmol) in the presence of PPh_3 (172 mg, 0.66 mmol) in THF (12 mL). After the mixture was stirred for 12 h at room temperature, the solvent was evaporated to dryness. The residue was extracted with pentane (10 mL × 3) and filtered. The pentane extract was evaporated to dryness under reduced pressure to give oily products. The ^{31}P{^{1}H} NMR spectrum showed formation of $Ru(CO)_2(PEt_3)_2(PPh_3)$ (major product) and $Ru(CO)_2(PEt_3)(PPh_3)_2$ (minor product), with a small amount of **1** and **3**. $Ru(CO)_2(PEt_3)_2(PPh_3)$: ^{31}P{^{1}H} NMR (C_6D_6, 23 °C) δ 31.8 (d, J_{PP} = 14 Hz, 2P, PEt_3), 45.9 (t, J_{PP} = 14 Hz, 1P, PPh_3). $Ru(CO)_2(PEt_3)(PPh_3)_2$: ^{31}P{^{1}H} NMR (C_6D_6, 23 °C) δ 27.7 (t, J_{PP} = 68 Hz, 1P, PEt_3), 50.4 (d, J_{PP} = 68 Hz, 2P, PPh_3).

Ru(H)$_2$(CO)$_2$(PEt$_3$)$_2$. A benzene (5 mL) solution of $Ru(CO)_2(PEt_3)_3$ (120 mg, 0.24 mmol) was placed in a Schlenk flask, and H_2 gas was passed through the solution overnight at room temperature with stirring. The solution, now colorless, was evaporated to dryness, and the residue was extracted with pentane (2 mL × 3). The pentane solution was concentrated to *ca*. 1 mL, then cooled to −78 °C, yielding colorless crystals. The crystalline complex melted into a colorless oil at room temperature; yield 61 mg (0.16 mmol, 66%). ^{1}H NMR (C_6D_6, 23 °C): δ −7.95 (t, J_{HP} = 24.0 Hz, 2H, Ru−*H*), 1.01 (tvt, J_{HP} = J_{HH} = 7.8 Hz, 18H, PCCH_3), 1.45 (qvt, J_{HH} = 7.6 Hz, J_{HP} = 3.2 Hz, 12H, PCH_2Me). ^{31}P{^{1}H} NMR (C_6D_6, 23 °C): δ 41.4 (s). IR (C_6D_6): ν_{CO} 1995, 1952 cm^{-1}. Anal. Calcd for $RuC_{14}H_{32}O_2P_2$: C, 42.52; H, 8.16. Found: C, 42.49; H, 7.82. This complex also can be synthesized from **5** or **6** with H_2 gas.

Ru(CO)$_3$(PEt$_3$)$_2$. $Ru(CO)_2(PEt_3)_3$ (100 mg, 0.20 mmol) was dissolved in benzene (5 mL), and carbon monoxide was passed through the solution at room temperature for 6 h with stirring. During this period, the solution color changed from pale yellow to colorless. The volatiles were removed under reduced pressure, and the white residue was extracted with pentane (2 mL × 3). After a small amount of insoluble material was filtered away, the solution was concentrated to *ca*. 1 mL and cooled to −40 °C, yielding colorless needles of the title compound; yield 67 mg (0.16 mmol, 81%). ^{1}H NMR (C_6D_6, 23 °C): δ 1.02 (dt, J_{HP} = 16.6 Hz, J_{HH} = 7.6 Hz, 18H, PCCH_3), 1.49 (qvt, J_{HH} = 7.6 Hz, J_{HP} = 3.7 Hz, 12H, PCH_2Me). ^{31}P{^{1}H} NMR (C_6D_6, 23 °C): δ 42.7 (s). IR (C_6D_6): ν_{CO} 1879 cm^{-1}. Anal. Calcd for $RuC_{15}H_{30}O_3P_2$: C, 42.75; H, 7.18. Found: C, 42.62; H, 6.85. This complex also can be synthesized from **5** or **6** with CO gas.

Ru(η^2-PhCCPh)(CO)$_2$(PEt$_3$)$_2$. (a) By Magnesium Reduction of *cis*,*cis*,*trans*-RuCl$_2$(CO)$_2$(PEt$_3$)$_2$. A THF (10 mL) solution of *cis*,*cis*,*trans*-$RuCl_2(CO)_2(PEt_3)_2$ (302 mg, 0.65 mmol) and diphenylacetylene (119 mg, 0.67 mmol) was added to a THF suspension of activated magnesium (16 mg, 0.65 mmol). The mixture was stirred for 12 h, and the solvent was evaporated to dryness. The resulting solid was extracted with pentane (10 mL × 3), concentrated to *ca*. 3 mL, and cooled to 0 °C, yielding two crops of yellow crystals of the title compound (300 mg, 80%). ^{1}H NMR (C_6D_6, 23 °C): δ 0.80 (m, 18H, PCCH_3), 1.24 (m, 12H, PCH_2Me), 7.06 (m, 2H, *p*-H), 7.29 (m, 4H, *m*-H), 8.09 (m, 4H, *o*-H). ^{31}P{^{1}H} NMR (C_6D_6, 23 °C): δ 30.1 (s). IR (C_6D_6): ν_{CO} 1954, 1892 cm^{-1}; ν_{CC} 1754 cm^{-1}. Anal. Calcd for $RuC_{28}H_{40}O_2P_2$: C, 58.83; H, 7.05. Found: C, 58.76; H, 6.92.

(b) From Ru(CO)$_2$(PEt$_3$)$_3$ and PhCCPh. To a solution of $Ru(CO)_2(PEt_3)_3$ (11 mg, 0.021 mmol) in C_6D_6 (0.5 mL) was added diphenylacetylene (6.0 mg, 0.034 mmol). The solution was kept stirring at room temperature. After 24 h of stirring, the ^{31}P NMR spectrum showed >95% conversion of **3** into Ru(η^2-PhCCPh)(CO)$_2$(PEt$_3$)$_2$ and free PEt_3. This complex also can be synthesized from **5** or **6** with PhCCPh.

Reaction of 3 with O$_2$. A C_6D_6 solution of $Ru(CO)_2(PEt_3)_3$ (15 mg, 0.029 mmol) was placed in an NMR tube with a Teflon stopcock. The headspace was degassed by a freeze−pump−thaw cycle, and a calibrated amount of O_2 gas (0.03 mmol) was introduced into the tube. Shaking the tube caused a solution color change from pale yellow to pale orange. The ^{31}P{^{1}H} NMR spectrum of this soluition, after 20 min, showed conversion to $Ru(CO_3)(CO)(PEt_3)_3$ with some other minor products as well as remaining starting complex. See text for detail. $Ru(CO_3)(CO)(PEt_3)_3$: ^{31}P{^{1}H} NMR (C_6D_6, 23 °C): δ 22.6 (d, J_{PP} = 22 Hz, 2P), 31.9 (t, J_{PP} = 22 Hz, 1P). IR (C_6D_6): ν_{CO} 1917 cm^{-1}, ν_{CO_3} 1669 cm^{-1}.

Ru(η^2-O_2)(CO)$_2$(PEt$_3$)$_2$. A solution of Ru(CO)$_2$(PEt$_3$)$_2$-(AsPh$_3$) (20 mg, 0.029 mmol) in C_6D_6 (0.5 mL) was placed in an NMR tube fitted with a Teflon stopcock. The solution was frozen in liquid N_2, the headspace was evacuated, and excess O_2 (1 atm) was introduced into the tube. On warming to room temperature and shaking the tube, the solution color changed immediately from pale yellow to pale orange. The remaining O_2 was then removed from the tube by a freeze−pump−thaw cycle. Although ^{1}H and ^{31}P{^{1}H} NMR and IR spectra showed clean conversion to Ru(η^2-O_2)(CO)$_2$(PEt$_3$)$_2$, the pure complex could not be isolated because of contamination with AsPh$_3$. ^{1}H NMR (C_6D_6, 20 °C): δ 0.93 (dt, $J_{HP} = J_{HH} = 7.6$ Hz, 18H, PCC*H*$_3$), 1.54 (qvt, $J_{HH} = 7.6$ Hz, $J_{HP} = 3.6$ Hz, 12H, PC*H*$_2$-Me). ^{31}P{^{1}H} NMR (C_6D_6, 20 °C): δ 33.8 (s). IR (C_6D_6): ν_{CO} 1995, 1925 cm^{-1}; ν_{OO} 839 cm^{-1}.

Ru(H)$_2$(CO)$_2$(P^{i}Pr$_2$Me)$_2$. A benzene (5 mL) solution of Ru(CO)$_2$(P^{i}Pr$_2$Me)$_3$ (122 mg, 0.22 mmol) was placed in a Schlenk flask, and H_2 gas was passed through the solution for 10 min at room temperature with stirring. The solution, now colorless, was evaporated to dryness, and the residue was extracted with pentane (2 mL × 3). The pentane solution was concentrated to *ca*. 1 mL, then cooled to −78 °C, yielding fine white needles; yield 66 mg (0.16 mmol, 71%). ^{1}H NMR (C_6D_6, 23 °C): δ −8.25 (t, $J_{HP} = 23.6$ Hz, 2H, Ru−*H*), 0.93 (dvt, $J_{HP} = J_{HH} = 7.0$ Hz, 12H, PCC*H*$_3$), 1.13 (br, 6H, PC*H*$_3$), 1.15 (dvt, $J_{HP} = J_{HH} = 7.0$ Hz, 12H, PCC*H*$_3$), 1.66 (m, 4H, PC*H*Me$_2$). ^{31}P{^{1}H} NMR (C_6D_6, 23 °C): δ 54.6 (s). IR (C_6D_6): ν_{CO} 1995, 1952 cm^{-1}. Anal. Calcd for $RuC_{16}H_{36}O_2P_2$: C, 45.38; H, 8.57. Found: C, 45.40; H, 8.17.

Ru(CO)$_3$(P^{i}Pr$_2$Me)$_2$. To a benzene (5 mL) solution of Ru-(CO)$_2$(P^{i}Pr$_2$Me)$_3$ (100 mg, 0.18 mmol) carbon monoxide was bubbled for 10 min at room temperature. The solution color changed from orange to colorless during this period. The volatiles were removed under reduced pressure, and the residue was extracted with pentane (3 mL × 3). The filtrate was concentrated to *ca*. 2 mL and cooled to −78 °C to give the title compound as colorless needles; yield 78 mg (0.17 mmol, 96%). ^{1}H NMR (C_6D_6, 23 °C): δ 0.98 (dvt, $J_{HP} = J_{HH} = 7.2$ Hz, 12H, PCC*H*$_3$), 1.16 (dvt, $J_{HP} = J_{HH} = 7.2$ Hz, 12H, PCC*H*$_3$), 1.19 (vt, $J_{HP} = 6.1$ Hz, 6H, PC*H*$_3$), 1.83 (m, 4H, PC*H*Me$_2$). ^{31}P-{^{1}H} NMR (C_6D_6, 23 °C): δ 51.1 (s). IR (C_6D_6): ν_{CO} 1869 cm^{-1}. Anal. Calcd for $RuC_{17}H_{34}O_3P_2$: C, 45.43; H, 7.62. Found: C, 45.31; H, 7.22.

Ru(η^2-PhCCPh)(CO)$_2$(P^{i}Pr$_2$Me)$_2$. Ru(CO)$_2$(P^{i}Pr$_2$Me)$_3$ (126 mg, 0.23 mmol) and diphenylacetylene (45 mg, 0.25 mmol) were dissolved into 5 mL of benzene, and the solution was stirred for 10 min at room temperature. The solvent was removed under reduced pressure, and the residue was extracted with pentane (3 mL × 3). The pentane solution was concentrated to *ca*. 4 mL and cooled to −40 °C to give yellow crystals; yield 129 mg (0.22 mmol, 95%). ^{1}H NMR (C_6D_6, 23 °C): δ 0.59 (vt, $J_{HP} = 2.7$ Hz, 6H, PC*H*$_3$), 0.89 (dvt, $J_{HP} = J_{HH} = 6.8$ Hz, 12H, PCC*H*$_3$), 1.02 (dvt, $J_{HP} = J_{HH} = 7.2$ Hz, 12H, PCC*H*$_3$), 1.72 (m, 4H, PC*H*Me$_2$), 7.04 (m, 2H, *p*-H), 7.29 (m, 4H, *m*-H), 8.02 (m, 4H, *o*-H). ^{31}P{^{1}H} NMR (C_6D_6, 23 °C): δ 40.0 (s). IR (C_6D_6): ν_{CO} 1956, 1894 cm^{-1}; ν_{CC} 1752 cm^{-1}. Anal. Calcd for $RuC_{30}H_{44}O_2P_2$: C, 60.09; H, 7.40. Found: C, 59.96; H, 7.28.

Ru(η^2-O_2)(CO)$_2$(P^{i}Pr$_2$Me)$_2$. Ru(CO)$_2$(P^{i}Pr$_2$Me)$_3$ (100 mg, 0.18 mmol) was placed in a Schlenk flask and dissolved in benzene (5 mL). The head space of the flask was evacuated by freeze−pump−thaw cycles, and O_2 gas (1 atm) was introduced to the flask. The solution was stirred at room temperature for 10 min, then evaporated to dryness. The residue was redissolved into pentane (5 mL). After a small amount of insoluble material was filtered away, the solution was concentrated to *ca*. 1 mL and cooled to −78 °C, yielding orange crystals of the product (68 mg, 0.15 mmol, 83%). ^{1}H NMR (C_6D_6, 23 °C): δ 0.94 (dvt, $J_{HP} = J_{HH} = 7.2$ Hz, 12H, PCC*H*$_3$), 1.03 (vt, $J_{HP} = 3.2$ Hz, 6H, PC*H*$_3$), 1.19 (dvt, $J_{HP} = J_{HH} = 7.2$ Hz, 12H, PCC*H*$_3$), 1.95 (m, 4H, PC*H*Me$_2$). ^{31}P{^{1}H} NMR (C_6D_6, 23 °C): δ 38.6 (s). IR (C_6D_6): ν_{CO} 1993, 1923 cm^{-1}; ν_{OO} 884 cm^{-1}. Anal. Calcd for $RuC_{16}H_{34}O_4P_2$: C, 42.38; H, 7.56. Found: C, 41.95; H, 7.26.

Table 1. Crystallographic Data for Ru(CO)$_2$(PEt$_3$)$_3$

formula: $C_{20}H_{45}O_2P_3Ru$	fw = 511.57
a = 14.229(2) Å	space group: $P2_1/n$
b = 11.216(1) Å	T = −171 °C
c = 16.572(2) Å	λ = 0.710 69 Å[a]
β = 104.17(1)°	ρ_{calcd} = 1.325 g cm^{-3}
V = 2564.45 Å^3	μ = 8.1 cm^{-1}
Z = 4	$R(F_o)$[b] = 0.0235
	$R_w(F_o)$[c] = 0.0244

[a] Graphite monochromator. [b] $R = \sum||F_o| - |F_c||/\sum|F_o|$. [c] $R_w = [\sum w(|F_o| - |F_c|)^2/\sum w|F_o|^2]^{1/2}$, where $w = 1/\sigma^2(|F_o|)$.

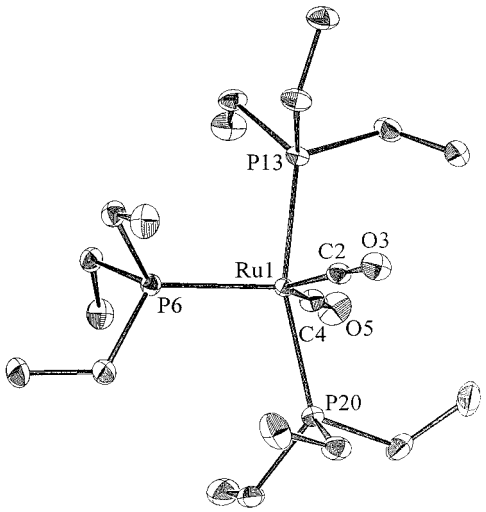

Figure 1. ORTEP drawing of Ru(CO)$_2$(PEt$_3$)$_3$, **3**, with selected atom labels.

X-ray Structure Determination. (a) Ru(CO)$_2$(PEt$_3$)$_3$. A single crystal was obtained by cleaving a large piece of the sample in a nitrogen atmosphere glovebag. The crystal was mounted using silicone grease, and it was then transferred to a goniostat where it was cooled to −171 °C for characterization and data collection. The compound is thermochromic, the bright yellow crystal becoming colorless at low temperature. A preliminary search for peaks and then analysis using the programs DIRAX and TRACER revealed a primitive monoclinic cell (Table 1). Following intensity data collection (6° < 2θ < 55°), the additional conditions $h + 1 = 2n$ for $h01$ and $k = 2n$ for $0k0$ uniquely determined the space group $P2_1/n$. Four standards measured every 300 data showed no signfiicant trends. The data were corrected for absorption (max and min factors: 0.818 and 0.924).

The structure was solved using a combination of direct methods (MULTAN78) and Fourier techniques. The position of the ruthenium atom was obtained from an initial E-map. The positions of the remaining non-hydrogen atoms were obtained from subsequent iterations of a least-squares refinement, followed by a difference Fourier calculation. All of ethyl groups of one of the three PEt$_3$ ligands were disordered, having a major (85% occupancy) and a minor (15% occupancy) orientation of each CH_2 moiety. Hydrogens were included in fixed calculated positions, with thermal parameters fixed at one plus the isotropic thermal parameter of the carbon to which it was bonded. Although only three of the non-hydrogen atoms have different positions in the two orientations of the disordered ligand, all 15 of the hydrogens have different positions. All were included with the appropriate occupancies and labels. In the final cycles of refinement, the non-hydrogen atoms were varied with anisotropic thermal parameters. The final difference map was featureless, the largest peak being 0.47 and the deepest hole −0.28 e/Å^3. The results are shown in Figure 1, Table 2, and the Supporting Information.

Table 2. Selected Bond Distances (Å) and Angles (deg) for $Ru(CO)_2(PEt_3)_3$

Ru(1)−P(6)	2.3761(5)	Ru(1)−C(4)	1.8964(19)
Ru(1)−P(13)	2.3422(5)	O(3)−C(2)	1.1679(24)
Ru(1)−P(20)	2.3524(5)	O(5)−C(4)	1.1613(24)
Ru(1)−C(2)	1.8883(19)		
P(6)−Ru(1)−P(13)	95.785(19)	P(13)−Ru(1)−C(4)	88.60(6)
P(6)−Ru(1)−P(20)	102.347(19)	P(20)−Ru(1)−C(2)	84.20(6)
P(6)−Ru(1)−C(2)	113.32(6)	P(20)−Ru(1)−C(4)	87.32(6)
P(6)−Ru(1)−C(4)	113.09(6)	C(2)−Ru(1)−C(4)	133.58(8)
P(13)−Ru(1)−P(20)	161.571(18)	Ru(1)−C(2)−O(3)	176.63(17)
P(13)−Ru(1)−C(2)	85.64(6)	Ru(1)−C(4)−O(5)	175.14(17)

Table 3. Crystallographic Data for $Ru(CO)_2(P^iPr_2Me)_3$

formula: $C_{23}H_{51}O_2P_3Ru$	fw = 553.65
a = 16.930(2) Å	space group: $P\bar{1}$
b = 17.932(2) Å	T = −173 °C
c = 9.540(1) Å	λ = 0.710 69 Å[a]
α = 93.27(1)°	ρ_{calcd} = 1.302 g cm^{-3}
β = 91.90(1)°	μ = 7.4 cm^{-1}
γ = 102.04(1)	$R(F_o)^b$ = 0.0345
V = 2824.88 Å^3	$R_w(F_o)^c$ = 0.0360
Z = 4	

[a] Graphite monochromator. [b] $R = \sum||F_o| - |F_c||/\sum|F_o|$. [c] $R_w = [\sum w(|F_o| - |F_c|)^2/\sum w|F_o|^2]^{1/2}$, where $w = 1/\sigma^2(|F_o|)$.

(b) $Ru(CO)_2(P^iPr_2Me)_3$. The complex is not only air-sensitive but also has a melting point slightly below room temperature. Fortunately, it is not sensitive to moisture and CO_2. The sample was handled on a dry-ice-cooled glass plate in a nitrogen atmosphere glovebag. A single crystal was obtained by cleaving a large piece of the sample, and it was then mounted on a glass fiber using silicone grease. The crystal was then transferred to a goniostat using a hand-held nitrogen cold stream, and it was then cooled to −173 °C for characterization and data collection ($6° < 2\theta < 45°$). A preliminary search for peaks revealed a triclinic cell (Table 3). An initial choice of space group $P\bar{1}$ was later proven correct by the successful solution of the structure. Four standards measured every 300 data showed no significant trends. The data were corrected for absorption (max and min factors: 0.862 and 0.924).

The structure was solved using a combination of direct methods (MULTAN78) and Fourier techniques. The positions of the ruthenium atoms were obtained from an initial E-map. The positions of the remaining non-hydrogen atoms were obtained from subsequent iterations of least-squares refinement, followed by a difference Fourier calculation. There were two molecules in the asymmetric unit. An isopropyl group and the methyl group on one of the phosphine ligands on Ru2 are disordered. The occupancies for the two orientations in the disorder were refined, and one orientation was dominant. After a small adjustment to normalize the total, the occupancies were 60.8% and 39.2%; these were fixed in the remaining refinement. Hydrogens were included in fixed calculated positions with thermal parameters fixed at one plus the isotropic thermal parameter of the carbon atom to which it was bonded.

In the final cycles of refinement, the non-hydrogen atoms were varied with anisotropic thermal parameters. The largest peak in the final difference map was 1.1 and the deepest hole was −0.5 e/Å^3. Results are shown in Figure 2, Table 4, and the Supporting Information

(c) $Ru(\eta^2\text{-PhC}{\equiv}\text{CPh})(CO)_2(PEt_3)_2$. A single crystal was obtained by cleaving a large piece of the sample in a nitrogen atmosphere glovebag. The crystal was mounted using silicone grease, and it was then transferred to a goniostat where it was cooled to −172 °C for characterization and data collection ($6° < 2\theta < 55°$). A preliminary search for peaks and then analysis using the programs DIRAX and TRACER revealed a C-centered monoclinic cell (Table 5). Following intensity data collection, the additional condition $1 = 2n$ for $h01$ limited the space group to *Cc* or *C*2/*c*. An initial choice of *C*2/*c* was later proven correct by the successful solution of the structure. Four standard reflections measured every 300 data showed no significant trends. The data were corrected for absorption; transmission factors ranged from 0.76 to 0.86.

The structure was solved using a combination of direct methods (MULTAN78) and Fourier techniques. The position of the ruthenium atom was obtained from an initial E-map. The positions of the remaining atoms, including nearly all of the hydrogens, were obtained from subsequent iterations of a least-squares refinement, followed by a difference Fourier calculation. All hydrogens were initially placed in idealized positions. In the final cycles of refinement, the non-hydrogen atoms were varied with anisotropic thermal parameters. The final difference map was featureless, the largest peak being 0.47 and the deepest hole −0.42 e/Å^3. Results are shown in Table 6 and the Supporting Information.

Computational Details. *Ab initio* calculations on the model system $Ru(CO)_2(PH_3)_3$ were carried out at the MP2 computational level. Effective core potentials were used to replace the 28 innermost electrons of the Ru atom,[14] as well as the 10 core electrons of each P atom.[15] The basis set is of valence double-ζ quality for all atoms,[14−16] supplemented with polarization functions on C, O, and P.[17] Geometry optimizations were performed within C_s symmetry, and Ru−P−H angles were restricted to a single value that was subsequently optimized.

In the IMOMM calculations, the quantum mechanics description was applied to the same model system used in the pure *ab initio* calculations described above: $Ru(CO)_2(PH_3)_3$. The *ab initio* computational level was exactly the same. For the molecular mechanics part, the MM3 force field was applied.[18] The torsional constants for the dihedral angles terminating at the Ru atom (i.e., Ru−P−C−C, Ru−P−C−H) were set to zero. The bond distances for the atoms linking the quantum mechanics and the molecular mechanics parts were frozen to 1.42 Å (P−H, *ab initio* description) and 1.843 Å (P−C, molecular mechanics description). Apart from this, IMOMM geometry optimizations were full, with no symmetry restrictions.

Results

Preparation of the Complexes. Magnesium reduction of *cis*,*cis*,*trans*-$RuCl_2(CO)_2(PPh_3)_2$ in THF in the presence of 1 equiv of PPh_3 gives clean conversion to $Ru(CO)_2(PPh_3)_3$, **1**, according to eq 2. Our spectroscopic

$$cct\text{-}RuCl_2(CO)_2L_2 + L + Mg \rightarrow Ru(CO)_2L_3 + MgCl_2 \quad (2)$$

$$L = PPh_3\ (\mathbf{1}),\ PMePh_2\ (\mathbf{2}),\ PEt_3\ (\mathbf{3}),\ P^iPr_2Me\ (\mathbf{4})$$

data for this molecule agree with those reported previously.[2,13] This new synthetic method is much simpler than the original synthetic route reported by Roper.[2] Dichloride complexes, $RuCl_2(CO)_2L_2$, are readily available from $RuCl_3{\cdot}nH_2O$ in high yield for a wide range of phosphines L.[10−12] Following this method makes it possible to synthesize analogous complexes with other phosphines, such as $PMePh_2$ (**2**), PEt_3 (**3**), and P^iPr_2Me (**4**). In all cases, reactions proceed cleanly and quanti-

(14) Hay, P. J.; Wadt, W. R. *J. Chem. Phys.* **1985**, *82*, 299.
(15) Wadt, W. R.; Hay, P. J. *J. Chem. Phys.* **1985**, *82*, 284.
(16) Hehre, W. J.; Ditchfield, R.; Pople, J. A. *J. Chem. Phys.* **1972**, *56*, 2257.
(17) (a) Krishnan, R.; Binkley, J. S.; Seeger, R.; Pople, J. A. *J. Chem. Phys.* **1980**, *72*, 650. (b) Francl, M. M.; Pietro, W. J.; Hehre, W. J.; Binkley, J. A.; Gordon, M. S.; DeFrees, D. J.; Pople, J. A. *J. Chem. Phys.* **1982**, *77*, 3654.
(18) Allinger, N. L. *MM3(92)*; QCPE: Bloomington, IN, 1992.

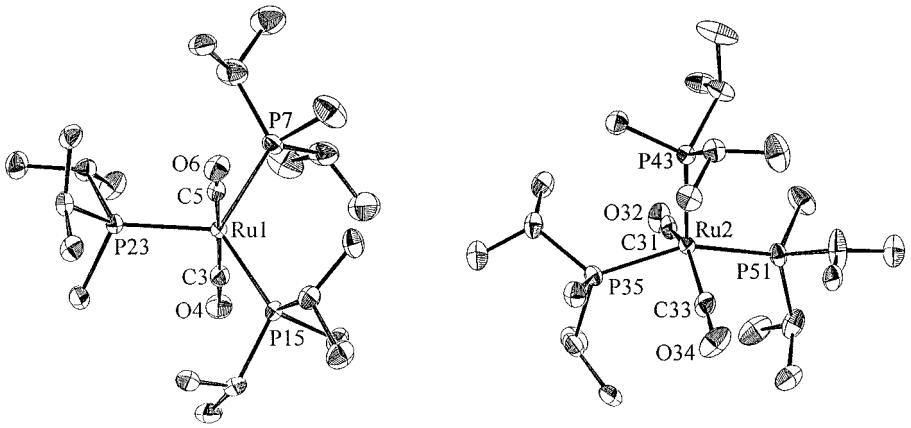

(a) (b)

Figure 2. ORTEP drawings of the two isomers of $Ru(CO)_2(P^iPr_2Me)_3$, **4**, with selected atom labels.

Table 4. Selected Bond Distances (Å) and Angles (deg) for $Ru(CO)_2(P^iPr_2Me)_3$

Ru(1)−P(7)	2.3423(12)	Ru(2)−P(51)	2.3589(11)
Ru(1)−P(15)	2.3400(11)	Ru(2)−C(31)	1.900(4)
Ru(1)−P(23)	2.3547(11)	Ru(2)−C(33)	1.902(4)
Ru(1)−C(3)	1.907(4)	O(4)−C(3)	1.156(5)
Ru(1)−C(5)	1.910(4)	O(6)−C(5)	1.147(5)
Ru(2)−P(35)	2.3594(11)	O(32)−C(31)	1.160(5)
Ru(2)−P(43)	2.3876(11)	O(34)−C(33)	1.154(5)
P(7)−Ru(1)−P(15)	116.81(4)	P(35)−Ru(2)−C(31)	88.44(12)
P(7)−Ru(1)−P(23)	115.33(4)	P(35)−Ru(2)−C(33)	85.41(13)
P(7)−Ru(1)−C(3)	95.82(12)	P(43)−Ru(2)−P(51)	105.31(4)
P(7)−Ru(1)−C(5)	90.04(13)	P(43)−Ru(2)−C(31)	106.72(13)
P(15)−Ru(1)−P(23)	127.81(4)	P(43)−Ru(2)−C(33)	106.59(14)
P(15)−Ru(1)−C(3)	86.61(12)	P(51)−Ru(2)−C(31)	84.24(12)
P(15)−Ru(1)−C(5)	88.46(12)	P(51)−Ru(2)−C(33)	87.34(13)
P(23)−Ru(1)−C(3)	86.20(12)	C(31)−Ru(2)−C(33)	146.68(18)
P(23)−Ru(1)−C(5)	93.63(12)	Ru(1)−C(3)−O(4)	176.9(3)
C(3)−Ru(1)−C(5)	173.61(17)	Ru(1)−C(5)−O(6)	178.0(3)
P(35)−Ru(2)−P(43)	100.30(4)	Ru(2)−C(31)−O(32)	177.6(3)
P(35)−Ru(2)−P(51)	154.39(4)	Ru(2)−C(33)−O(34)	177.3(4)

Table 5. Crystallographic Data for $Ru(PhC_2Ph)(CO)_2(PEt_3)_2$

formula: $C_{28}H_{45}O_2P_2Ru$	fw = 571.64
a = 19.353(2) Å	space group: $C2/c$
b = 11.368(1) Å	T = −172 °C
c = 26.558(3) Å	λ = 0.710 69 Å[a]
β = 103.45(1)°	ρ_{calcd} = 1.336 g cm^{-3}
V = 5682.69 Å^3	μ = 6.86 cm^{-1}
Z = 8	$R(F_o)^b$ = 0.0313
	$R_w(F_o)^c$ = 0.0320

[a] Graphite monochromator. [b] $R = \sum||F_o| - |F_c||/\sum|F_o|$. [c] $R_w = [\sum w(|F_o| - |F_c|)^2/\sum w|F_o|^2]^{1/2}$, where $w = 1/\sigma^2(|F_o|)$.

tatively, with the solution color change from colorless to yellow. The isolated yield of the complexes is in the range of 83−93%, depending on the solubility and crystallinity of the complexes.

Reduction of *cis*,*cis*,*trans*-$RuCl_2(CO)_2(PEt_3)_2$ in the presence of equimolar PPh_3 according to eq 3 for 12 h gives $Ru(CO)_2(PEt_3)_2(PPh_3)$ as the main product. This

$$cct\text{-}RuCl_2(CO)_2(PEt_3)_2 + L' + Mg \rightarrow Ru(CO)_2(PEt_3)_2L' + MgCl_2 \quad (3)$$

$$L' = PPh_3,\ P(2\text{-furyl})_3\ (\mathbf{5}),\ AsPh_3\ (\mathbf{6})$$

assignment comes from the observed AM_2 pattern(s) in the ^{31}P NMR spectrum and also knowing the ^{31}P NMR chemical shifts of $Ru(CO)_2(PPh_3)_3$ (at 50.4 ppm) and of

Table 6. Selected Bond Distances (Å) and Angles (deg) for $Ru(PhC_2Ph)(CO)_2(PEt_3)_2$

Ru(1)−P(20)	2.3640(6)	O(17)−C(16)	1.152(3)
Ru(1)−P(27)	2.3632(7)	O(19)−C(18)	1.151(3)
Ru(1)−C(2)	2.1538(23)	C(2)−C(3)	1.286(3)
Ru(1)−C(3)	2.1538(22)	C(2)−C(10)	1.461(3)
Ru(1)−C(16)	1.9014(24)	C(3)−C(4)	1.461(3)
Ru(1)−C(18)	1.9017(25)		
P(20)−Ru(1)−P(27)	175.158(20)	C(3)−Ru(1)−C(16)	143.70(10)
P(20)−Ru(1)−C(2)	87.39(6)	C(3)−Ru(1)−C(18)	113.15(10)
P(20)−Ru(1)−C(3)	88.54(6)	C(16)−Ru(1)−C(18)	103.14(10)
P(20)−Ru(1)−C(16)	90.81(7)	Ru(1)−C(2)−C(3)	72.63(14)
P(20)−Ru(1)−C(18)	90.71(8)	Ru(1)−C(2)−C(10)	138.03(17)
P(27)−Ru(1)−C(2)	87.85(6)	C(3)−C(2)−C(10)	149.28(23)
P(27)−Ru(1)−C(3)	87.05(6)	Ru(1)−C(3)−C(2)	72.63(14)
P(27)−Ru(1)−C(16)	91.57(7)	Ru(1)−C(3)−C(4)	139.40(17)
P(27)−Ru(1)−C(18)	92.85(8)	C(2)−C(3)−C(4)	147.94(23)
C(2)−Ru(1)−C(3)	34.74(9)	Ru(1)−C(16)−O(17)	177.97(23)
C(2)−Ru(1)−C(16)	108.98(10)	Ru(1)−C(18)−O(19)	177.45(23)
C(2)−Ru(1)−C(18)	147.84(10)		

$Ru(CO)_2(PEt_3)_3$ (at 31.2 ppm). When the reduction is carried out with a Ru:PPh_3 ratio of 1:1.7, the formerly major AM_2 $^{31}P\{^1H\}$ NMR pattern observed from the 1:1 molar ratio and assigned to $Ru(CO)_2(PEt_3)_2(PPh_3)$ is now smaller and the formerly minor AM_2 pattern assigned to $Ru(CO)_2(PEt_3)(PPh_3)_2$ is now larger. The fact that reduction of *cis*,*cis*,*trans*-$RuCl_2(CO)_2(PEt_3)_2$ in the presence of PPh_3 can lead to a product containing more than one PPh_3 and less than two PEt_3 suggests possible ligand redistribution can be a complicating factor; that is, trapping of the transient reduction product $Ru(CO)_2(PEt_3)_2$ is not the only process taking place. To test the possibility of ligand redistribution subsequent to forming Ru(0), $Ru(CO)_2(PPh_3)_3$ was reacted with equimolar PEt_3 for 1 h at 23 °C in THF. This yields all possible $Ru(CO)_2(PEt_3)_n(PPh_3)_{3-n}$ species, together with free PPh_3. This confirms the hypothesis that pure $Ru(CO)_2(PEt_3)_2(PPh_3)$ could undergo ligand redistribution even in the absence of added free PR_3. The complex $Ru(CO)_2(PPh_3)_3$ is particularly susceptible to reaction with PEt_3, since it has been suggested to participate in the equilibrium (eq 4). Because of their complexity, we did not

$$Ru(CO)_2L_3 \underset{k_{-1}}{\overset{k_1}{\rightleftharpoons}} Ru(CO)_2L_2 + L \quad (4)$$

investigate in detail the kinetics or thermodynamics of these redistributions.

Tris(2-furyl)phosphine (PFr_3) is a phosphine with a steric profile close to that of PPh_3,[19] but with much less σ-basicity.[20] It is thus a promising candidate as a leaving group from an Ru(CO)$_2$L$_2$L′ species. In addition, the electronic property of this phosphine as a very weak σ-donor may avoid the sort of ligand redistribution in a Ru(CO)$_2$L$_2$L′ species, which was observed in the PEt_3/PPh_3 system as described above. In order to have selectivity in ligand loss from Ru(CO)$_2$L$_2$L′, we chose PEt_3 as the tightly binding ligand L. As expected, reduction according to eq 3 proceeds cleanly within 12 h. Recrystallization of the pentane extract gives a mixed phosphine complex Ru(CO)$_2$(PEt_3)$_2$(PFr_3), **5**, in pure form in 83% yield. Similarly, the phosphine/arsine complex Ru(CO)$_2$(PEt_3)$_2$($AsPh_3$), **6**, was prepared from *cis*,*cis*,*trans*-RuCl$_2$(CO)$_2$(PEt_3)$_2$ and $AsPh_3$ in 68% isolated yield. The lower yield of **6** can be attributed to the low crystallinity of **6**, since an NMR-scale experiment showed almost quantitative conversion of *cis*,*cis*,-*trans*-RuCl$_2$(CO)$_2$(PEt_3)$_2$ into **6**.

Spectroscopic and Crystallographic Characterization of the Complexes. All of the complexes Ru(CO)$_2$L$_3$ (**1**−**4**, L = PPh_3, $PMePh_2$, PEt_3, P^iPr_2Me) show only one ^{31}P NMR resonance at room temperature, which could be taken to indicate structure **A**. However,

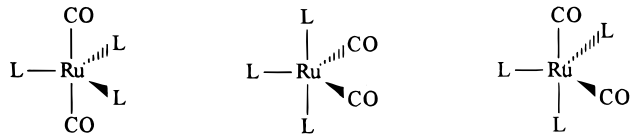

rapid fluxionality of the molecules in solution is expected for these five-coordinate complexes, so infrared spectroscopy (a "faster" technique) is a more reliable method for structural assignment of these complexes. Only one ν_{CO} band is predicted for the *trans* structure **A**, two CO absorptions with unequal intensity for the *cis* structure **B**, and two ν_{CO} bands with approximately equal intensity for **C**. The IR spectrum of **2** in C_6D_6, which shows two strong ν_{CO} bands, is inconsistent with structure **A**. The IR intensities of complex **2** can be used to calculate the angle between the two CO diatomic oscillators of 117°,[21] which is surely too large for an axial and equatorial location of two carbonyls (∼90°, structure **C**) but is consistent with structure **B**. The ^{31}P{^{1}H} NMR spectrum of **2** in toluene at −93 °C shows considerable broadening of the signal (δ 28.3, $w_{1/2} \approx 250$ Hz); this chemical shift is almost the same as that at 23 °C. Unfortunately, then, it is not possible to halt this fluxionality, which time-averages the axial and equatorial phosphine sites of **B**. The observed broadening can be attributed to slow rotation about the Ru−P and P−C bonds in the ligands in **2** at this temperature.[22] Complex **3** also shows similar NMR and IR characteristics to those of **2**.

The structural conclusions from the spectroscopic data described above were confirmed by single-crystal X-ray diffraction of **3**. As shown in Figure 1, in the solid state, two carbonyls of complex **3** occupy equatorial positions. These equatorial ligands have a C2−Ru1−C4 angle of 133.58(8)°, which is somewhat above the ideal 120° angle. The P6−Ru−C2/4 angles are then identical at 113.32(6)° and 113.09(6)°. The two axial phosphines bend away from the equatorial phosphine (angles 95.785(19)° and 102.347(19)°), so that the (*trans*) P13−Ru1−P20 angle is only 161.571(18)°. The equatorial P6−Ru1 distance, 2.3761(5) Å, is statistically significantly longer than the axial P−Ru distances (2.35 Å average). The equatorial and one of the axial phosphines have only one CH_3 group anti to the Ru−P bond, but the second axial phosphine has no CH_3 anti to the Ru−P bond. Both axial PEt_3 groups are nearly staggered with respect to the equatorial Ru(CO)$_2$P subunit.

The structure of Roper's complex **1** has been assigned as **A**, based on its IR spectrum,[2] which is different from those of **2** and **3**. This structural difference might originate in the steric properties of the phosphine ligands. Indeed, the IR spectrum of **4** in pentane shows a strong band at 1867 cm^{-1}, consistent with the structure **A** expected for a phosphine, P^iPr_2Me, of cone angle 146°, which is nearly identical with that of PPh_3 (145°).[23] However, this band in the P^iPr_2Me complex has a significant shoulder at *ca.* 1850 cm^{-1}, which is too high a frequency and excessively intense to be a ^{13}CO isotopomer of the *trans* carbonyl species. If this band is due to an isomer, it should be possible to alter the mole fractions of each by selective solvation. Any second isomer **B** or **C** has a dipole moment. Therefore, it should be favored in a polar solvent. In fact, the IR spectra of **4** in THF or ethanol show increasing amounts of the lower frequency band and also greater separations of this band from that of the *trans* CO isomer.[9] If the assignment of the lower energy band mentioned above is correct, there must also be a symmetric stretch at about 60 cm^{-1} higher frequency. Assuming a C−Ru−C angle of about 147° (based on an X-ray structure determination of **4**, *vide infra*), this band should have an intensity only 9% of that of the asymmetric stretch. Although we note a weak band in the expected location, its anticipated weakness makes assignment uncertain. Stronger back-donation is expected for the second isomer than that in the *trans* CO isomer. The observation of ν_{CO} of the second isomer at lower frequency than that of the *trans* CO isomer is consistent with this structural assignment.

Against this background of solution behavior, the X-ray structure of crystalline **4** is especially interesting. The unit cell contains equal amounts of two crystallographically-independent molecules. One is quite accurately a *trans* CO TBP (structure **A**) with idealized C_{3v} symmetry (Figure 2a). The second is not well-described as a trigonal bipyramid. Instead, it is better described as a square pyramid (Figure 2b). This is a somewhat subtle point since both **B** (TBP) and **D** (square pyramid) have C_{2v} symmetry. Perhaps the

(19) There is no report on the steric profile of tris(2-furyl)phosphine. However, the cone angle of tri(*N*-pyrrolyl)phosphine, which also has five-membered heteroaryl substituents, has been reported as identical with that of PPh_3. Moloy, K. G.; Petersen, J. L. *J. Am. Chem. Soc.* **1995**, *117*, 7696.

(20) (a) Allen, D. W.; Taylor, B. F. *J. Chem. Soc., Dalton Trans.* **1982**, 51. (b) Allen, D. W.; Bell, N. A.; Fong, S. T.; March, L. A.; Nowell, I. W. *Inorg. Chim. Acta* **1985**, *99*, 157.

(21) Cotton, F. A.; Wilkinson, G. *Advanced Inorganic Chemistry*, 5th ed.; Wiley: New York, 1988; p 1935.

(22) Notheis, J. U.; Heyn, R. H.; Caulton, K. G. *Inorg. Chim. Acta* **1995**, *229*, 187.

(23) (a) Tolman, C. A. *Chem. Rev.* **1977**, *77*, 313. (b) White, D.; Coville, N. J. *Adv. Organomet. Chem.* **1994**, *36*, 95.

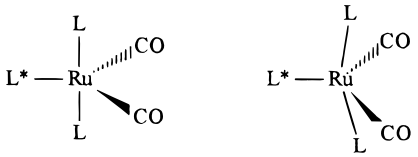

B **D**

decisive factor favoring the square pyramidal assignment is thus the increase of the C−Ru−C angle from the expected 120−130° value in a TBP to 147°. Clearly, the structure adopted is controlled by an attempt to minimize L/L repulsion, and apparently, increasing only the L−Ru−L* angle leads to higher energy than also distorting the C−Ru−C angle to a square pyramidal form. This concerted displacement follows the conventional path of Berry pseudorotation. Since both isomers exist in the solid state, we have attempted to investigate the solid state IR spectrum. However, the complex **4** is a solid with a low melting point (mp = *ca.* 15 °C) and our attempt was unsuccessful.

Finding the two isomers of **4**, both in the solid state and in solution, prompted us to reinvestigate Roper's complex **1**, whose geometry was described as structure **A**.[2] Indeed, the solution IR spectrum of **1** in C_6D_6 shows a small signal at 1856 cm^{-1} in addition to an originally reported CO absorption at 1908 cm^{-1}. The expected second ν_{CO} band of the minor isomer is estimated at *ca.* 1910 cm^{-1}, where it overlaps with the strong signal of the main isomer. Again, ν_{CO} of the minor isomer (with bent OC−Ru−CO) is observed at a lower frequency than that of the major isomer (with *trans* CO ligands), as shown for complex **4**.

Although attempted synthesis of $Ru(CO)_2(PEt_3)_2(PPh_3)$ leads to a ligand redistribution to form a mixture of $Ru(CO)_2(PEt_3)_2(PPh_3)$ and $Ru(CO)_2(PEt_3)(PPh_3)_2$, their ^{31}P NMR spectra give quite interesting structural information of these molecules. In the ^{31}P NMR spectra, each of the complexes is observed as an AM_2 pattern. However, there is a huge difference between their $^2J_{PP}$ coupling constants: 14 Hz for $Ru(CO)_2(PEt_3)_2(PPh_3)$, which is thus attributed to structure **B**, and 68 Hz for $Ru(CO)_2(PEt_3)(PPh_3)_2$, which is attributed to structure **A**. This structural change is caused by the averaged cone angle of the three phosphines in $Ru(CO)_2(PEt_3)_2(PPh_3)$ being 136° while that in $Ru(CO)_2(PEt_3)(PPh_3)_2$ is 141°.[23] These observations strongly support the influence of steric bulk of the phosphines in $Ru(CO)_2(phosphine)_3$ on the geometry of the complex.

Similarly, the $^{31}P\{^1H\}$ NMR spectrum of **5** (L′ = PFr_3) shows an AM_2 pattern. The chemical shift of PFr_3 in this compound is shifted 61 ppm downfield from that of pure PFr_3 (δ −76.5 in C_6D_6 at 23 °C), which proves that it is bound to Ru by a phosphorus atom and not by the furyl ring. The $^2J_{PP}$ coupling constant, 24 Hz, is consistent with a 90° P−Ru−P′ angle of structure **B** with the PFr_3 at an equatorial position and inconsistent with structure **A** (∼80 Hz expected). Two CO stretches with unequal intensity are seen in the IR spectrum at 1900 and 1842 cm^{-1} in C_6D_6, confirming structure **B**. Although these values are low enough to be consistent with zero-valent Ru, they are shifted to somewhat higher frequency compared to those of $Ru(CO)_2(PEt_3)_3$ (1883 and 1825 cm^{-1}). The weaker σ-donor character of PFr_3 decreases the electron density at the Ru center, and thus diminishes back-donation to the carbonyl ligands. The π-accepting properties of PFr_3 may also contribute to the coordination of PFr_3 in an equatorial plane. The molecule is persistent to ligand redistribution, which was observed on the PEt_3/PPh_3 system described above; heating a toluene solution of $Ru(CO)_2(PEt_3)_2(PFr_3)$ up to 110 °C does not show any ligand redistribution products.

Spectroscopic characteristics of **6** (L′ = $AsPh_3$) are very similar to those of **5**. In the $^{31}P\{^1H\}$ NMR spectrum, **6** shows only one singlet and even at −90 °C the signal is observed as a sharp resonance at the same chemical shift. These observations are consistent with the two phosphines in **6** being equivalent. In the IR spectrum of **6**, two CO stretches are shown with unequal intensity. All of these data suggest the structure of **6** as **B**, with triphenylarsine at the third equatorial position.

Theoretical Calculations of Isomer Preference. It thus seems that small-to-medium-sized phosphines yield an isomer where the carbonyls adopt equatorial sites, while large phosphines (e.g., PPh_3) adopt a structure which minimizes phosphine/phosphine repulsion: the *trans* dicarbonyl isomer. This indicates that the reported electronic preference of CO for an equatorial site[24] is small enough to be ultimately dominated by steric effects, but the solid state structure of $Ru(CO)_2(PEt_3)_3$ does agree with an earlier molecular orbital analysis which found back-donation most efficient in the equatorial sites of a TBP.

Full optimization by *ab initio* calculations at the MP2 level were carried out for $Ru(CO)_2(PH_3)_3$. Three energetically-close minima were located with geometries similar to **A**, **B**, and **C**. The two most stable isomers, essentially (i.e., within 0.2 kcal·mol^{-1}) isoenergetic, were found to have two equatorial CO ligands, isomer **B**, and one equatorial and one axial CO ligand, isomer **C**. The third isomer, **A**, with two axial CO ligands was calculated to be only 3 kcal·mol^{-1} above the two other isomers. This work will focus on isomers **A** and **B**. Isomer **C** is not considered further because of the *fac* arrangement of three bulky ligands.

The most relevant structural parameters of structures **A** and **B** are shown in Scheme 1 (*trans* and *cis*). The structure of the *trans* CO isomer, optimized in C_s symmetry, has essentially a TBP geometry. The structure of the *cis* CO isomer deviates only modestly from TBP geometry. The main deviation is the opening of the angle between the two CO ligands (128.5°) and a slight bending of the phosphine toward this enlarged angle (P−Ru−P = 174.1°). The bond lengths have some interesting patterns. The longest Ru−P bond is obtained for the equatorial phosphine in the *cis* isomer. The Ru−C bond is shorter and accordingly the C-O bond is longer for the *cis* isomer. This bond length pattern is in accord with a well-established fact:[24] σ-donor ligands (phosphine) make the weakest bond at the equatorial site, while, in contrast, π-acceptors (CO) make the strongest bond.

While the geometry pattern is in agreement with the commonly-accepted effect of a π-acceptor ligand at the equatorial site, the energy pattern is surprising. Such a small difference in energy (3 kcal·mol^{-1}) between the

(24) Rossi, A. R.; Hoffmann, R. *Inorg. Chem.* **1975**, *14*, 365.

Scheme 1

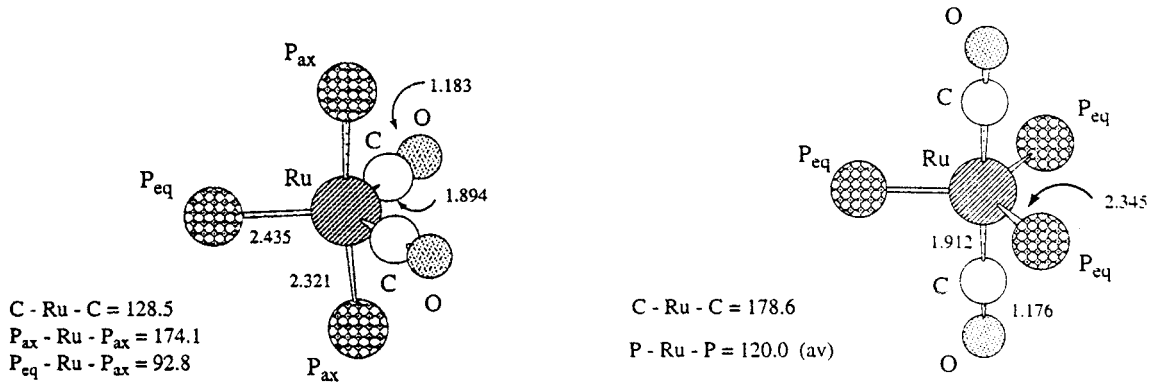

Scheme 2

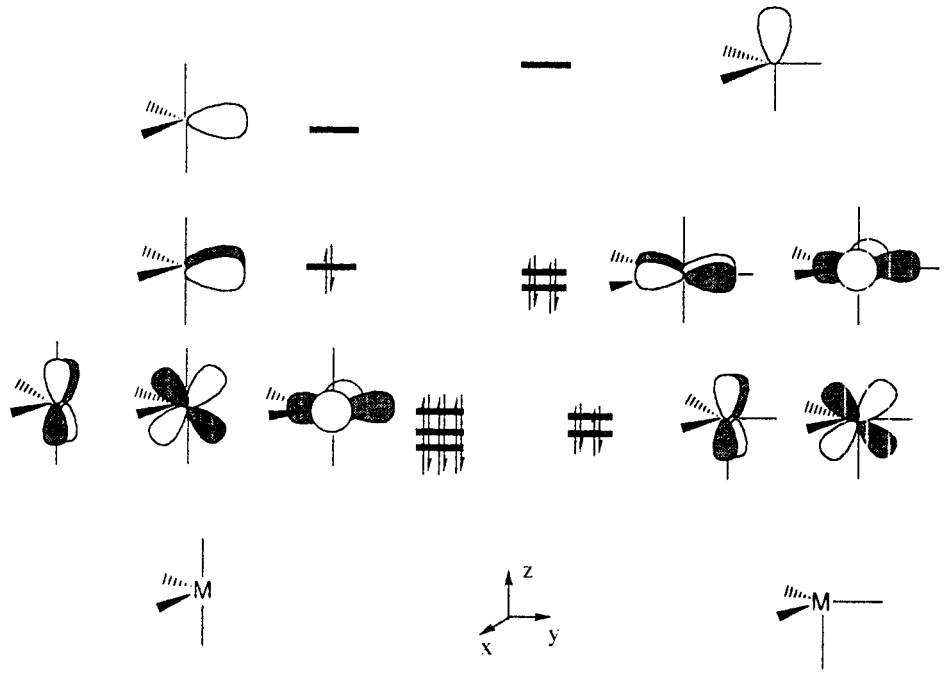

cis and *trans* structures suggest that there is no strong site preference for the CO ligand. Since this result was surprising, it was necessary to determine if this pattern would also hold for a monocarbonyl complex and also if it is characteristic of other π-acids.

The geometry of the model species Ru(CO)$(PH_3)_4$ was therefore optimized. Two minima were located, corresponding to the two different isomers with an equatorial and axial CO ligand. As in the dicarbonyl system, a small difference in energy (2 kcal·mol^{-1}) in favor of the equatorial CO isomer is obtained. Therefore, a monocarbonyl also shows the same effect as the dicarbonyl complex. However, this absence of electronic site preference for the equatorial site cannot be generalized to all π-accepting ligands. For example, calculations were carried out on Ru$(PH_3)_4(C_2H_4)$. In this system, the only minimum is found for ethylene at the equatorial site and lying in the equatorial plane. All of the other structures, including that with axial ethylene, are about 20 kcal·mol^{-1} higher in energy.

It remains to be understood why CO and C_2H_4 ligands behave differently. This surprising result can be understood by considering the interactions of a ML_4 fragment with a ligand to form the TBP species. If the ligand is positioned at the equatorial site, the ML_4 fragment has a C_{2v} symmetry, while if it is at the axial site, it has a C_{3v} symmetry. The orbitals of the C_{2v} metal fragment, which have the proper symmetry to interact with the HOMO 5σ of CO, are the occupied $x^2 - y^2$ orbital and the empty LUMO made of a mixture of p_y and s orbitals.[25] In the case of a C_{3v} metal fragment, there is only one empty metal orbital (made of d_{z^2}, p_z, and s) to interact with the HOMO of CO (Scheme 2). The occupied $x^2 - y^2$ orbital interacts in a four-electron destabilizing way with the ligand attached at the equatorial site. Such destabilization is absent when the ligand is attached at the axial site. The back-donation from the metal into the two π^*_{CO} of the ligand is larger when associated with the HOMO of the C_{2v} metal fragment. Thus, while back-donation clearly favors the equatorial site, a σ interaction disfavors it because of the four-electron repulsion. This four-electron repulsion is large in the case of CO since the HOMO directly points toward $x^2 - y^2$. It is of lesser importance in the case of olefin since the π orbital is closer to the nodal planes of $x^2 - y^2$. Thus, the behavior of CO is strongly influenced by the σ M−CO interactions and, therefore, shows some similarities in behavior with a phosphine. This difference between ethylene and CO should be kept

(25) Albright, T. A.; Burdett, J. K.; Whangbo, M.-H. In *Orbital Interactions in Chemistry*; Wiley: New York, 1985.

Table 7. Values of Selected Bond Distances and Bond Angles Optimized for Complex 3A at the IMOMM(MP2:MM3) Computational Level

Ru−P(2)	2.363	Ru−C(5)	1.910
Ru−P(3)	2.370	Ru−C(6)	1.903
Ru−P(4)	2.361		
P(2)−Ru−P(3)	116.3	P(4)−Ru−C(5)	91.5
P(2)−Ru−P(4)	122.7	P(2)−Ru−C(6)	87.8
P(3)−Ru−P(4)	121.0	P(3)−Ru−C(6)	91.0
P(2)−Ru−C(5)	90.4	P(4)−Ru−C(6)	89.5
P(3)−Ru−C(5)	89.9	C(5)−Ru−C(6)	178.2

Table 8. Values of Selected Bond Distances and Bond Angles Optimized for Complex 3B at the IMOMM(MP2:MM3) Computational Level. X-ray Values are Included in Parentheses for Comparison

Ru−P(6)	2.480 (2.376)	Ru−C(4)	1.891 (1.896)
Ru−P(13)	2.347 (2.342)	Ru−C(2)	1.889 (1.888)
Ru−P(20)	2.349 (2.352)		
P(6)−Ru−P(13)	97.8 (95.8)	P(6)−Ru−C(2)	110.1 (113.3)
P(6)−Ru−P(20)	102.3 (102.3)	P(13)−Ru−P(20)	159.9 (161.6)
P(6)−Ru−C(4)	113.2 (113.1)	C(4)−Ru−C(2)	136.7 (133.6)

in mind when the different behavior by these π-accepting ligands is considered.

Theoretical Evaluation of Steric *vs* Electronic Effects. The pure *ab initio* calculations on the model $Ru(CO)_2(PH_3)_3$ system presented in the previous section provide a satisfactory characterization of the electronic effects, but they can only provide qualitative suggestions on what might be the steric effects. These steric effects were therefore quantitatively assessed through theoretical calculations with the IMOMM computational scheme. This is a recently developed method that allows a geometry optimization of the equilibrium and transition state geometries of large molecular systems by integrating molecular orbital (MO) calculations for a small model system and molecular mechanics (MM) calculations for the remainder of the system.[26] In this method, the energy of the real system is expressed as a sum of the MO energy of the small model system and the MM energy of the real system, excluding the part already calculated with the MO method. Using this energy and its gradient with respect to the nuclear coordinates, one can fully optimize the structures of the real system. With a proper choice of the model system, this computational scheme is able to provide *ab initio* quality results on large systems at a price only slightly higher than that of the *ab initio* calculations on model systems. The method has been successfully applied to the study of some transition metal systems, like $Pt(PR_3)_2H_2$[27] and $OsO_4(NR_3)$.[28]

IMOMM calculations were carried out on complexes **3** ($Ru(CO)_2(PEt_3)_3$) and **4** ($Ru(CO)_2(P^iPr_2Me)_3$), those for which there are X-ray structures available. These calculations yield two local minima for each of the systems, corresponding to isomers **A** and **B**. Experimental X-ray structures are available for species **3B**, **4A**, and **4B**, while **3A** had not been previously identified. The most significant parameters of the optimized structures are presented in Tables 7−10, together with the corresponding experimental values. With only the exception of some Ru−P distances (in particular, Ru−P_{eq} for isomer **B**), which have errors as large as 0.1 Å, agreement between the computed and experimental bond distances and angles is very good. The improvement of bond angles with respect to pure *ab initio* calculations on the model system is clear. The IMOMM computed value for the P_{ax}−Ru−P_{ax} angle, which was 171.1° for the model system, is 159.9° for complex **3** (X-ray, 161.6°) and 157.4° for complex **4B** (X-ray, 154.4°). The experimental difference among bond angles between the three equatorial phosphine ligands in complex **4A** (127.8°, 116.8°, and 115.3°) was absent from the *ab initio* calculation on the model system but is reproduced by the IMOMM calculation, with values of 127.1°, 117.4°, and 115.5°.

Table 9. Values of Selected Bond Distances and Bond Angles Optimized for Complex 4A at the IMOMM(MP2:MM3) Computational Level. X-ray Values are Included in the Parentheses for Comparison

Ru−P(15)	2.371 (2.340)	Ru−C(3)	1.904 (1.907)
Ru−P(23)	2.392 (2.355)	Ru−C(5)	1.908 (1.910)
Ru−P(7)	2.395 (2.342)		
P(15)−Ru−P(23)	127.1 (127.8)	P(7)−Ru−C(3)	94.5 (95.8)
P(15)−Ru−P(7)	117.4 (116.8)	P(15)−Ru−C(5)	88.4 (88.5)
P(23)−Ru−P(7)	115.5 (115.3)	P(23)−Ru−C(5)	92.3 (93.6)
P(15)−Ru−C(3)	87.2 (86.6)	P(7)−Ru−C(5)	90.8 (90.0)
P(23)−Ru−C(3)	87.4 (86.2)	C(3)−Ru−C(5)	174.3 (173.6)

Table 10. Values of Selected Bond Distances and Bond Angles Optimized for Complex 4B at the IMOMM(MP2:MM3) Computational Level. X-ray Values are Included in Parentheses for Comparison

Ru−P(43)	2.476 (2.388)	Ru−C(31)	1.892 (1.900)
Ru−P(35)	2.372 (2.359)	Ru−C(33)	1.898 (1.902)
Ru−P(51)	2.364 (2.359)		
P(43)−Ru−P(35)	102.2 (105.3)	P(43)−Ru−C(33)	105.9 (106.6)
P(43)−Ru−P(51)	100.3 (100.3)	P(35)−Ru−P(51)	157.4 (154.4)
P(43)−Ru−C(31)	108.6 (106.7)	C(31)−Ru−C(33)	145.6 (146.7)

Even more interesting than the agreement of the IMOMM predictions with experimental geometries are the energetics these calculations provide. Complex **3**, isomer **B**, the only one existing in the crystal, is computed to be more stable than isomer **A** by 3.0 kcal·mol^{-1}. The relationship between the two isomers is reversed for complex **4**, with **A** being 2.8 kcal·mol^{-1} more stable than **B**. Electronic effects associated with the quantum mechanics part of IMOMM always favor the isomeric form **B**, with the two carbonyl ligands in equatorial positions, by 3.1 kcal·mol^{-1} in the case of **3** and by 1.7 kcal·mol^{-1} in the case of **4**. Steric effects, represented by the molecular mechanics part of IMOMM, mark the difference between **3** and **4**. Steric effects always favor the isomeric form **A**, with the two carbonyl ligands in axial positions, but they do it by quite different magnitudes: the preference is quantified as 0.1 kcal·mol^{-1} for complex **3** and 4.5 kcal·mol^{-1} for complex **4**. Therefore, the picture emerging from these calculations is quite clear. There is an electronic preference for the placement of the π-acidic carbonyl ligands in equatorial positions (isomer **B**) though, quantitatively, this preference is always smaller than 5 kcal·mol^{-1} and definitely smaller than was *a priori* expected.[24] There is a steric preference toward the placement of the bulkier phosphine ligands in the equatorial positions (isomer **A**), the weight of this

(26) Maseras, F.; Morokuma, K. *J. Comput. Chem.* **1995**, *16*, 1170.
(27) Matsubara, T.; Maseras, F.; Koga, N.; Morokuma, K. *J. Phys. Chem.* **1996**, *100*, 2573.
(28) Ujaque, G.; Maseras, F.; Lledós, A. *Theor. Chim. Acta* **1996**, *94*, 67.

preference depending on the nature of the phosphine ligand. In small phosphines, like PEt_3, this steric effect is negligible and isomer **B** is the more stable form. In larger phosphines, like P^iPr_2Me, steric effects are strong enough to invert the small electronic preference for isomer **B** and isomer **A** becomes the more stable form.

A final aspect of the IMOMM calculation deserving discussion concerns the Ru−P_{eq} distance in the isomeric form **B**. This particular bond has some significance, since it is the likely candidate to be broken in the phosphine dissociation process that is the necessary preliminary step for all the reactivity of these complexes.[5] On the one hand, it certainly presents the longest Ru−P distance, as one may expect from the weaker bond. It does so in all of our tests, both experimental (X-ray on **3** and **4**) and theoretical (pure *ab initio* on model system, IMOMM on **3** and **4**), with this lengthening being overestimated in the theoretical calculations. This simple correlation between bond strength and bond length is, however, not so straightforward as it may appear. This is the only possible conclusion from the comparison between complexes **3B** and **4B**. It is clear both from theory and experiment that this isomeric form **B** is destabilized with respect to form **A** in the case of complex **4**. One should, therefore, expect a weaker bond in **4B**, as it is indeed proven by its larger reactivity. However, the Ru−P_{eq} distances are practically the same in **3B** and **4B** (**3** longer than **4** by 0.012 Å in X-ray; **4** longer than **3** by 0.004 Å in IMOMM). However, the increase in the phosphine cone angle is manifested in an increase of the P_{ax}−Ru−P_{eq} angle (**3**, X-ray, 95.8°; IMOMM, 97.8°. **4**, X-ray, 100.3°; IMOMM 100.3°).

These theoretical results prompted us to reevaluate our spectral data in search of evidence for a second (or a third) isomer in the experimental system. Since NMR spectra can be obscured by rapid fluxional averaging of signals from more than one isomer, we reevaluated our IR spectra. The two strong bands in the spectrum of **3** in pentane (assigned to isomer with structure **B**) are accompanied by an additional weak absorption at 1860 cm^{-1} (Figure 3), which we assign to the isomer of structure **A**. Consistent with the lack of dipole moment of the *trans* dicarbonyl **3A**, there is less of it at equilibrium in the more polar solvent THF.

Reactivity of the Complexes. The reactivity of the new complexes was studied for selected complexes, **3**, **4**, **5**, and **6**, with H_2, CO, PhCCPh, and O_2. Complexes **3**, **5**, and **6** all react with H_2, CO, and PhC≡CPh to give $Ru(H)_2(CO)_2(PEt_3)_2$, $Ru(CO)_3(PEt_3)_2$, and Ru(η^2-PhC≡CPh)$(CO)_2(PEt_3)_2$, respectively, together with formation of free PEt_3 for **3**, PFr_3 for **5**, and $AsPh_3$ for **6**. In all cases, the reactions are clean and proceed quantitatively, judging from their $^{31}P\{^1H\}$ NMR spectra. The reactions are very slow for **3** and **5**, and their half-lives are on the order of hours. Complex **6** is much more reactive than **3** and **5**; all of the reactions mentioned above are complete within 10 min. All of these reactions can be explained as proceeding with an initial dissociation of a phosphine or arsine ligand from the complexes to give the common transient $Ru(CO)_2(PEt_3)_2$. In cases of reactions with **5** or **6**, the dissociation of PFr_3 from **5** and $AsPh_3$ from **6** is highly selective; no production of free PEt_3 is observed. To test for such a dissociative equilibrium, we have recorded the $^{31}P\{^1H\}$ NMR spectrum of **5** in the presence of equimolar PFr_3 at 80 °C. There is no broadening of each signal (or coalescence). Thus, any such dissociation of PFr_3 from **5** is too slow to observe by this NMR technique. However, direct confirmation of such a dissociation will be discussed later. It is also noteworthy that this solution shows no detectable production of $Ru(CO)_2(PEt_3)(PFr_3)_2$ under these conditions. However, we cannot simply conclude from these results that tris(2-furyl)phosphine is more weakly binding to the Ru than PEt_3 (*vide infra*).

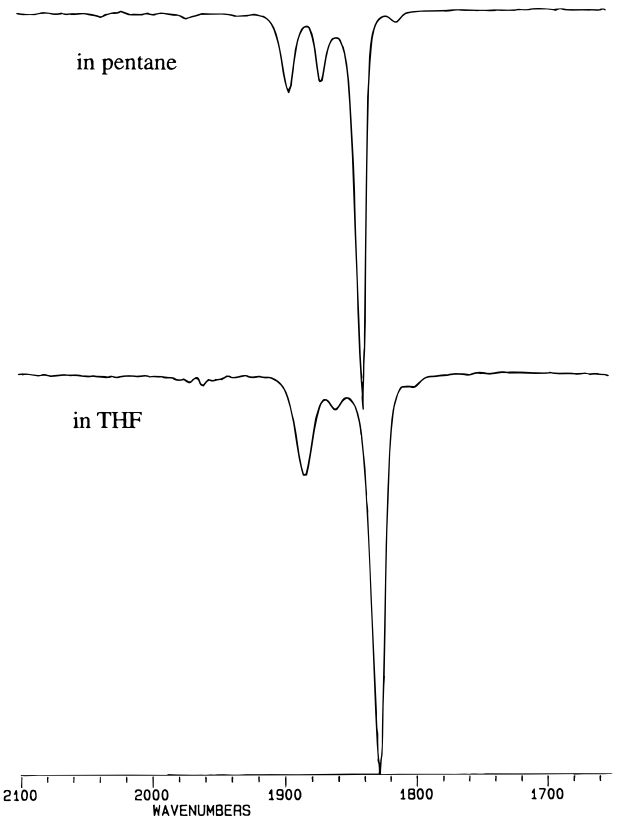

Figure 3. Infrared spectra (ν_{CO} region) of $Ru(CO)_2(PEt_3)_3$, **3**, in pentane and THF.

The solid state structure of Ru(η^2-PhC≡CPh)$(CO)_2$-$(PEt_3)_2$ is shown in Figure 4.[29] The molecule adopts a structure in which the two phosphines are *trans*, and the two carbonyls, Ru, and the *entire* PhCCPh ligand are coplanar. The structure might be described as trigonal bipyramidal with axial phosphines, but the angle between the two carbonyls is only 103.14(10)°, which more closely resembles an octahedral angle of Ru(II). The molecule has very close to C_{2v} symmetry. The Ru−C16 and Ru−C18 distances are equal, as are the Ru−C2 and Ru−C3 distances. Consistent with the alkyne acting as only a two-electron donor, the Ru−C2/3 distances are long (2.15 Å) and the C2−C3 distance is lengthened only modestly (to 1.286(3) Å) from that in the free alkyne (1.204(12) Å).[30] The alkyne phenyl rings are bent back to C2−C3−C4 = 147.9(2)° and C3−C2−C10 = 149.3(2)°. The three ethyl groups on each phosphorus adopt the common conformation with one methyl

(29) Gagné, M. R.; Takats, J. *Organometallics* **1988**, *7*, 561. Birdwhistell, K. R.; Tonker, T. L.; Templeton, J. L. *J. Am. Chem. Soc.* **1987**, *109*, 1401. Marinelli, G.; Streib, W. E.; Huffman, J. C.; Caulton, K. G.; Gagné, M. R.; Takats, J.; Dartiguenave, M.; Chardon, C.; Jackson, S. A.; Eisenstein, O. *Polyhedron* **1990**, *19*, 1867.

(30) Indiana University Molecular Structure Center Report No. 7774, available from the Chemistry Library, Indiana University.

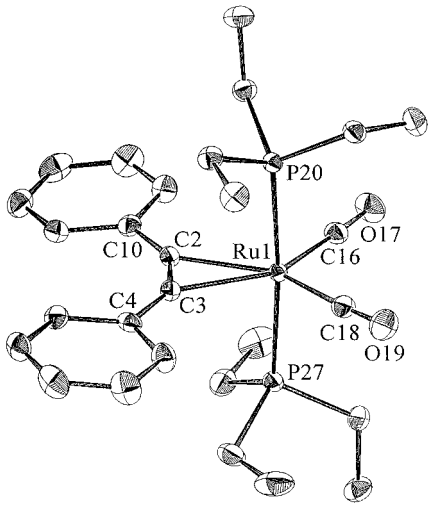

Figure 4. ORTEP drawing of $Ru(\eta^2\text{-}PhCCPh)(CO)_2(PEt_3)_2$ with selected atom labels.

anti to the Ru−P bond and the other two methyls nearly in the plane of the three CH_2 groups. The conformation about each Ru−P bond makes the ethyl groups staggered with respect to all of the Ru−C bonds.

The reactions of complexes **3**, **5**, and **6** with O_2 are quite different from each other. A benzene solution of **6** reacts immediately with dioxygen gas (immediate color change) to give $Ru(\eta^2\text{-}O_2)(CO)_2(PEt_3)_2$. Although the spectroscopic data (^1H and $^{31}P\{^1H\}$ NMR and IR) showed the quantitative conversion to the dioxygen adduct, isolation of the product in pure form could not be achieved due to contamination by released $AsPh_3$. The reaction of **3** and O_2 is more complex; the $^{31}P\{^1H\}$ NMR spectrum of the initial reaction mixture shows two sets of AM_2 patterns (**III** and **I**) and a signal of Et_3PO in addition to resonances of some other minor products (one of which is $Ru(\eta^2\text{-}O_2)(CO)_2(PEt_3)_2$). The AM_2 patterns indicate formation of tris(triethylphosphine) species, one of which, **III**, isomerizes to the other (**I**) in 2 days at room temperature (see Scheme 3).[31] The IR spectrum of this solution shows a strong absorption in the Ru−CO region at 1917 cm^{-1} and a weaker band at 1669 cm^{-1}, which is consistent with structure **I**. Another stereoisomer, **II**, is possible for this species; however, a facial arrangement of the bulkier ligands, triethylphosphines, is not probable since this orientation of the three phosphines was distinctly less favorable (could not be detected) in $Ru(CO)_2(PEt_3)_3$ (structure **C**). Structure **I** also has a push/pull interaction between carbonate oxygen and CO, which is less effective in **II**. As for the other initial product, we propose structure **III**. A mixture of $Ru(\eta^2\text{-}O_2)(CO)_2(PEt_3)_2$ and PEt_3 does not form **I**, which indicates that **I** does not form via phosphine dissociation from **3**. The different reaction patterns between **3** and **6** toward O_2 suggest that tighter binding of the three phosphine ligands is important for formation of the carbonate complex. Similar carbonate complexes are reported for reactions between $Ru(CO)_2(L_3)$ and O_2, where L_3 are tridentate phosphines. In $Ru(CO)_2(L_3)$, the tridentate phosphines resist dissociation due to the chelate effect.[7ab,32] A reaction between **5** and O_2 gives many products and is impossible to characterize.

(31) Roundhill, D. M. *Comprehensive Coordination Chemistry*; Pergamon Press: New York, 1987; Vol. 5, p 463. Collman, J. P. *Acc. Chem. Res.* **1968**, *1*, 136. Curtis, M. D.; Han, K. R. *Inorg. Chem.* **1985**, *24*, 378. Roper, W. R. *J. Organomet. Chem.* **1986**, *300*, 167.

Complex **4**, which has different structures (square pyramid and *trans*-TBP) than **3** (*cis*- and *trans*-TBP), shows much higher reactivity than **3**. However, its reaction patterns toward H_2, CO, and PhC≡CPh are identical to those of **3** to give $Ru(H)_2(CO)_2(P^iPr_2Me)_2$, $Ru(CO)_3(P^iPr_2Me)_2$, and $Ru(\eta^2\text{-}PhC{\equiv}CPh)(CO)_2(P^iPr_2Me)_2$, respectively, together with dissociated equimolar P^iPr_2Me. It also reacts with O_2 to give $Ru(\eta^2\text{-}O_2)(CO)_2(P^iPr_2Me)_2$ and P^iPr_2Me. All of these reactions are very clean and quite fast (they are finished within an observation time of 10 min).

Tris(2-furyl)phosphine: A Strong π-Acceptor. The unusual phosphine tris(2-furyl)phosphine was initially employed in **5** because of its extremely weak σ-basicity.[20] Thus, it was expected that PFr_3 in **5** would be a leaving group from **5** and that introduction of PFr_3 into the complex would enhance its reactivity. Judging from the reaction patterns of **5** toward H_2, CO, and PhCCPh (*vide supra*), this first objective has been realized. However, is complex **5** more reactive than **3**? During the preliminary reaction study described above, we could not detect any dramatic reactivity enhancement in **5** *vs* **3**. The reaction progress of **3** and **5** toward

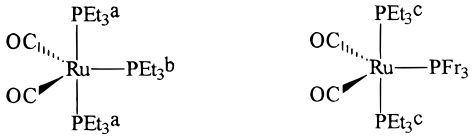

3 **5**

PhCCPh was therefore monitored by $^{31}P\{^1H\}$ NMR, and the results are shown in Figure 5. Quite unpredictably, the PFr_3/PEt_3 complex, **5**, is somewhat less reactive than **3**. Since the reaction between the isolable four-coordinate complex $Ru(CO)_2(P^tBu_2Me)_2$ and PhCCPh proceeds in the time of mixing,[6] a probable common intermediate from **3** or **5**, $Ru(CO)_2(PEt_3)_2$, should react with PhCCPh immediately. Thus, the rate-determining step of the reaction can be assumed to be phosphine dissociation from **3** or **5**. The lower reactivity of **5** indicates that PFr_3 in **5** binds tighter than PEt_3 in **3**. Combined with the weak σ-base character of PFr_3, these observations can be used to propose a stronger π-acidity of PFr_3. However, this point, the tighter coordination of PFr_3, is a little bit confusing, since the dissociation of PFr_3 from **5** is highly selective. The X-ray crystal structure of **3** and the *ab initio* calculations on $Ru(CO)_2(PH_3)_3$ show that the $Ru-P_{eq}$ bond is longer than the $Ru-P_{ax}$ distance, i.e., $RuPEt_3^b$ is the weakest Ru−P bond in **3**. Thus, the order of the bond strength in **3** and **5** can be estimated as $Ru-PEt_3^b < Ru-PFr_3 < Ru-PEt_3^c$. The second inequality makes PFr_3 the leaving group from **5**; the first inequality makes **5** less reactive than **3**.

Dissociation of a Phosphine from $Ru(CO)_2L_3$. Although it has been suggested that **1** undergoes phosphine dissociation in solution, as shown in eq 4, and its reactivity has supported this idea, there is no direct evidence of this equilibrium.[2] We have tried to detect evidence of eq 4 by monitoring the $^{31}P\{^1H\}$ NMR spectra of $Ru(CO)_2L_3$ in the presence of free L for L = PEt_3 and P^iPr_2Me. In the case of L = PEt_3, the signals for both

(32) Christian, D. F.; Roper, W. R. *J. Chem. Soc., Chem. Commun.* **1971**, 1271.

Scheme 3

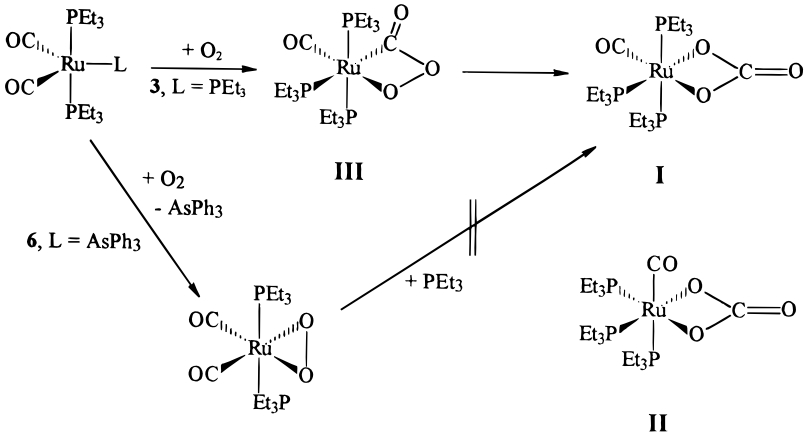

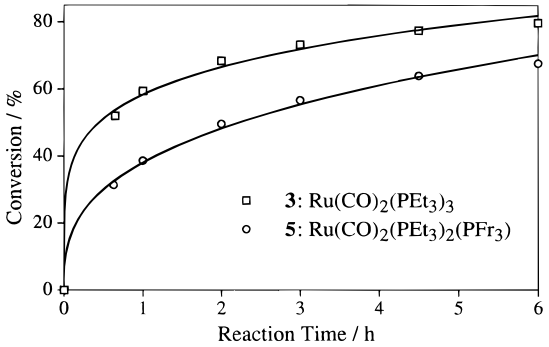

Figure 5. Progress of the reactions between PhCCPh (5.9 × 10^{-2} mmol) and **3** or **5** (5.9 × 10^{-2} mmol) in C_6D_6 (0.5 mL) at 20 °C.

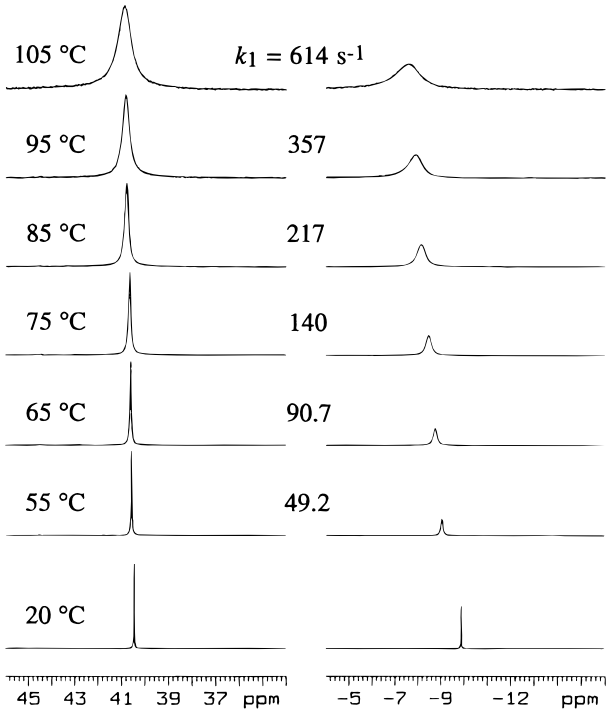

Figure 6. Observed variable-temperature 122 MHz ^{31}P NMR spectra of a mixture of $Ru(CO)_2(P^iPr_2Me)_3$, **4** (δ 40.4, 0.14 mmol), and P^iPr_2Me ($\delta \sim -9$, 0.21 mmol) in toluene-d_8 (0.7 mL). The rate constants for phosphine loss from **4** are shown.

3 and free PEt_3 are sharp even at 110 °C in toluene and do not show any obvious line broadening in their NMR spectrum. This is consistent with a low reactivity of **3** toward H_2, CO, and PhCCPh to give bis(triethylphosphine) complexes. However, $^{31}P\{^1H\}$ NMR signals of a mixture of **4**, which is the most reactive complex in our hands, and free P^iPr_2Me show increased broadening at higher temperatures, as shown in Figure 6. For the mixture of **4** and P^iPr_2Me, the line width of free P^iPr_2-Me is first-order in [**4**]. In addition, the line width of the $^{31}P\{^1H\}$ NMR signal of **4** at 85 °C is independent of the concentration of **4** and of added free P^iPr_2Me. Furthermore, spin-saturation transfer was observed between the signals of **4** and free P^iPr_2Me by ^{31}P NMR at 75 °C. Saturation of the free phosphine resonance led to a considerable decrease in the intensity of the resonance of coordinated phosphine. All of these observations confirm the dissociative mechanism (eq 4) for line broadening. The rate constants k_1 were determined over 10 °C increments between 55 and 105 °C from the line widths of the free P^iPr_2Me.[33] An Eyring plot of these data is linear, and the activation parameters for the dissociation of the phosphine from **4** are $\Delta H^‡ = 11.3 \pm 0.4$ kcal·mol^{-1}, $\Delta S^‡ = -16.7 \pm 1.0$ cal·mol^{-1}·K^{-1}, and $\Delta G^‡$ (at 85 °C) = 17.3 ± 0.8 kcal·mol^{-1}. The negative $\Delta S^‡$ is unexpected for a dissociative process, and it contributes significantly to raising the modest $\Delta H^‡$ to a larger $\Delta G^‡$. We suggest that this negative $\Delta S^‡$ comes in part from the need to first rearrange the less crowded *trans* dicarbonyl **A** to structure **D**, Scheme 4. The greater crowding in **D** will contribute to a negative $\Delta S^‡$ as will additional bending of L toward L* as **D** proceeds toward the transition state (we know the structure of $Ru(CO)_2L_2$).[5] For example, it has been shown that $\Delta S°$ for a similar rearrangement (of $Os(CO)_2(C_2F_4)(PPh_3)_2$) is −14.3 cal·mol^{-1}·K^{-1}.[34] Apparently, after **D** is formed, there is only a minimum release of entropy until point ‡ is reached. The $\Delta H^‡$ and $\Delta G^‡$ obtained here lie in the range of those reported for the H_2 dissociation from dihydrogen complexes.[35] Dihydrogen represents one of

(33) The rate constants, k_1, were calculated from the following equation: $k_1 = \pi R[\Delta^{-1}/(\pi T_2)]$, where R is P^iPr_2Me(free)/**4** molar ratio, Δ is the free phosphine line width, and T_2 is the spin−spin relaxation time of the free phosphine resonance.

(34) Burrell, A. K.; Clark, G. R.; Rickard, C. E. F.; Roper, W. R.; Ware, D. C. *J. Organomet. Chem.* **1990**, *398*, 133.

(35) (a) Zhang, K.; Gonzalez, A. A.; Hoff, C. D. *J. Am. Chem. Soc.* **1989**, *111*, 3627. (b) Millar, J. M.; Kastrup, R. V.; Melchior, M. T.; Howath, I. T.; Hoff, C. D.; Crabtree, R. H. *J. Am. Chem. Soc.* **1990**, *112*, 9643. (c) Halper, J.; Cai, L. S.; Desrosiers, P. J.; Lin, Z. R. *J. Chem. Soc., Dalton Trans.* **1991**, 717. (d) Gusev, D.; Kuhlman, R. L.; Renkema, K. B.; Eisenstein, O.; Caulton, K. G. *Inorg. Chem.* **1996**, *35*, 6775.

Scheme 4

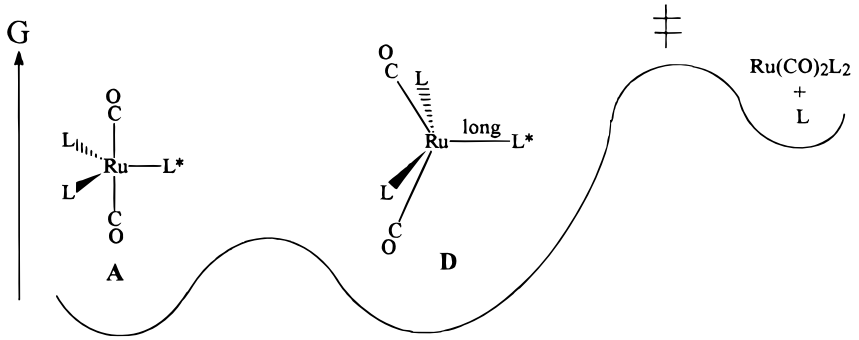

the weakest ligands in transition metal chemistry. The kinetic parameters obtained here (being an upper limit on the dissociation energy) indicate how easy the phosphine dissociation is in **4**. In contrast, $\Delta H^{\ddagger}$ for loss of CO from $Ru(CO)_5$ is 27.6 kcal·mol^{-1}.[36]

Discussion

The complexes $Ru(CO)_2L_2L'$ participate in either an X or Y equilibrium, in solution, and this is very dependent on the steric and electronic properties of the phosphines. The order of the steric properties (cone angle) of the phosphines[23] which we employed in this study is P^{i}Pr$_2$Me (146°) > PPh_3 (145°) > $(PPh_3)_2(PEt_3)$ (141°, average) > $(PPh_3)(PEt_3)_2$ (136°, average) ≈ $PMePh_2$ (136°) > PEt_3 (132°). This order clearly explains the relationship between the steric characteristics of the phosphines and the structure of the complexes; the first three give equilibrium X, the latter three are Y. In

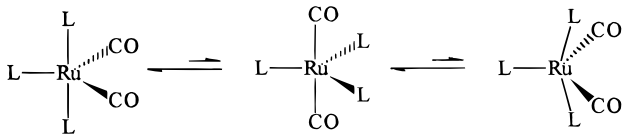

Y **X**

contrast, the electronic properties (pK_a value shown below) of the phosphine do not fit with the structural behavior: P^{i}Pr$_2$Me[37] > PEt_3 (8.69) > $(PPh_3)(PEt_3)_2$ (6.70, average) > $(PPh_3)_2(PEt_3)$ (4.72, average) > $PMePh_2$ (4.57) > PPh_3 (2.73). It is known that the equatorial sites in a five-coordinate d^8 complex permit the greatest back-donation.[24] Thus, the strongest π-acceptor will occupy equatorial sites (Y) until phosphine/phosphine steric repulsion becomes intolerable (e.g., PPh_3 = L = L′), and then structure X is preferred. However, the electronic site preference is small in the case of CO, and thus, it is relatively easy to manipulate the structures by steric control only. A comprehensive study of $M(CO)_4(ER_3)$ species (M = Fe, Ru, O_5; E = P, As, Sb; R = Me, Ph) has shown an equilibrium in solution between axial- and equatorial-ER_3 isomers and related these to both steric and electronic factors.[38]

The varied reactivity of $Ru(CO)_2L_2L'$ with O_2 is proposed to depend on the relative ability of the four-coordinate species $Ru(CO)_2L_2$ (which leads immediately to $Ru(O_2)(CO)_2L_2$) and also the ease of (one-electron) oxidation of intact $Ru(CO)_2L_2L'$. We propose that the relatively electron-rich $Ru(CO)_2(PEt_3)_3$ (which only slowly loses PEt_3) reacts in part by electron transfer with O_2 and that the geminate pair $[Ru(CO)_2(PEt_3)_3^{+\bullet}; O_2^{-\bullet}]$ collapses to form the peroxycarbonate **III**. The presence of the peroxy linkage makes **III** metastable, and it ultimately rearranges to carbonate.

This work has shown the continuum of behavior, both structural and reactivity, which can come from systematic variation of the phosphine identity in $Ru(CO)_2L_3$. Our synthetic method also allows detection of further subtle features which arise in mixed phosphine or phosphine/arsine species $Ru(CO)_2L_2L'$. While it was always clear that different structures were of similar energy for a five-coordinate complex, there were only very rarely instances of two structures coexisting at detectable levels and those were only in the solid state, where intramolecular preferences could be subject to solid state packing effects. This is the first study where systematic modification of the groups L and L′ permit mapping of the changeover of the preferred isomer from electronically to sterically dictated. For example, we show how a *cis* isomer can be sterically destabilized and a *trans* isomer results. What could not have been anticipated, however, is that destabilizing the *cis*-TBP form gives rise to not one but two alternatives, the *trans* and the distorted *cis*. Moreover, the cone angle similarity between P^{i}Pr$_2$Me and PPh_3 led to reinvestigation and the discovery that **1** is not simply a *trans* isomer. The phenomenon of multiple isomers in solution is general. The detected structure of the distorted *cis* isomer relied wholly on the coexistence of this form with the *trans* isomer in the crystal studied by X-ray diffraction. This has the additional benefit of showing how a bulky phosphine can increase the thermal dissociative reactivity of Ru(0). Moreover, these results, with phosphines of cone angle less than 146°, provide a context for better understanding why P^{t}Bu$_2$Me, with cone angle 161°, destabilizes a $Ru(CO)_2L_3$ species to the point where $Ru(CO)_2(P^tBu_2Me)_2$ can be isolated and will not interact with P^{t}Bu$_2$Me.[6] The resulting four-coordinate, zero-valent Ru species then shows a remarkably high but also sterically-selective reactivity.

Thus, even for a very "ordinary" phosphine like PEt_3, our studies show the coexistence of two isomers of $Ru(CO)_2L_3$. As the phosphine becomes larger, two isomers are still present, but their coordination geometry is considerably different from trigonal bipyramidal. Since these results apply even to the frequently employed

(36) Hastings, W. R.; Roussel, M. R.; Baird, M. C. *J. Chem. Soc., Dalton Trans.* **1990**, 203.

(37) Although the pK_a value of P^{i}Pr$_2$Me has not been reported, there is a report postulating that P^{i}Pr$_2$Me is more basic than PEt_3. See: Vasteg, S.; Heil, B.; Markó, L. *J. Mol. Catal.* **1979**, *5*, 189.

(38) Martin, L. R.; Einstein, F. W. B.; Pomeroy, R. K. *Inorg. Chem.* **1985**, *24*, 2777.

phosphine PPh_3, the generality and significance of the present results seems established. Several other examples of coexistence of several TBP isomers have been reported previously. Thus, $Os(CO)_2(C_2H_4)_3$ exists as diaxial dicarbonyl and axial/equatorial dicarbonyl isomers,[39] and $Os(C_2F_4)(CO)_2(PPh_3)_2$ coexists[34] as diequatorial and diaxial dicarbonyl isomers which do not coalesce by ^{31}P NMR at 25 °C. The work reported here shows the dramatic impact of the phosphine identity on the chemical reactivity of these molecules.

We began this project with the objective of finding some compound $Ru(CO)_2L_2L'$ which would serve as a "stable" (long shelf-life as a solid) precursor on dissolving (by eq 4) to four-coordinate, reactive $Ru(CO)_2L_2$ for ligands L where the isolation of this 16-electron species eluded us, due to unfavorable thermodynamics.[6] This was, in fact, the special utility of Roper's complex $Ru(CO)_2(PPh_3)_3$. This goal has been achieved in the form of $Ru(CO)_2(PEt_3)_2(AsPh_3)$ and $Ru(CO)_2(P^iPr_2Me)_3$, while $Ru(CO)_2(PEt_3)_3$ stands as a useful comparison compound in terms of its greatly reduced reactivity (in the absence of outer sphere electron transfer, with a reagent like O_2). The study of $Ru(CO)_2(PEt_3)_2[P(2\text{-furyl})_3]$ reveals that the $P(2\text{-furyl})_3$ ligand binds more tightly than might have been predicted.

Acknowledgment. F.M. thanks the CNRS for a research associate position. N.G.-P.'s stay in Montpellier was financed by the European Community via the Human Capital and Mobility Program (CHRX-CT93-0152). The U.S./France Collaboration (K.G.C./O.E.) was financed by a bilateral NSF/CNRS (PICS) program. We thank Professor Masahiko Saburi of Saitama Institute of Technology and Johnson Mathey/Aesar for material support.

Supporting Information Available: Tables of crystallographic data, fractional coordinates, and thermal parameters and crystal structures for $[Ru(CO)_2(PEt_3)_3]$, $[Ru(CO)_2(P^iPr_2Me)]$, and $[Ru(PhC_2Ph)(CO)_2(PEt_3)_2]$ (15 pages). Ordering information is given on any current masthead page.

OM9700775

(39) Kiel, G.-Y.; Takats, J.; Grevels, F.-W. *J. Am. Chem. Soc.* **1987**, *109*, 2227.